Electronic Supplementary Materials for

# Significant Effects of Counteranions on the Anticancer Activity of Iridium(III) Complexes

Hairong Zhang,[a] Lihua Guo,[a]* Zhenzhen Tian,[a] Meng Tian,[a] Shumiao Zhang,[a] Zhishan Xu,[ab] Peiwei Gong,[a] Xiaofeng Zheng,[a] Jia Zhao,[a] Zhe Liu[a]*

[a] *Institute of Anticancer Agents Development and Theranostic Application, The Key Laboratory of Life-Organic Analysis and Key Laboratory of Pharmaceutical Intermediates and Analysis of Natural Medicine, Department of Chemistry and Chemical Engineering, Qufu Normal University, Qufu 273165, China.*

[b] *Department of Chemistry and Chemical Engineering, Shandong Normal University, Jinan 250014, China.*

*Corresponding author. Email: liuzheqd@163.com; Email: guolihua@qfnu.edu.cn.

Supporting information includes the experimental details and data.

## Supporting Information

**EXPERIMENTAL SECTION..... S2-S5**
**Tables S1-S11 …..... S6-S10**
**Figure S1..... S8**
**Figure S2 ……..…..... S9**
**Figures S3-S34 ..... S10-S26**

# EXPERIMENTAL SECTION

## Syntheses.

**Materials**. $IrCl_3 \cdot nH_2O$, 2,3,4,5-tetramethyl-2-cyclopentenone (95%), 4-bromo-biphenyl, butyllithium solution (1.6 M in hexane), $AgBF_4$, $NaSbF_6$, $AgCF_3SO_3$, $NH_4BPh_4$, NaBAF, 2, 2′-bipyridine, ammonium hexafluorophosphate, anhydrous $MgSO_4$, n-hexane, diethyl ether, ethanol, dry THF. $Cp^{xbiph}H$ ($Cp^{biph}$ =$\eta^5$-$C_5Me_4C_6H_4C_6H_5$), $[Cp^{biph}IrCl_2]_2$ and complex **2** were synthesized according to the reported methods.[1] For the biological experiments, phosphate-buffered saline (PBS), penicillin/streptomycin mixture, fetal bovine serum, trypsin/EDTA and DMEM medium were purchased from Sangon Biotech.. Testing compounds was dissolved in DMSO and diluted with the tissue culture medium before use.

**[$Cp^{biph}$Ir(bpy)Cl]Cl** (**1**). A solution of $[Cp^{biph}IrCl_2]_2$ (43.0 mg, 0.04 mmol) and 2, 2′-bipyridine (15.6 mg, 0.1 mmol) in 60 mL anhydrous methanol was stirred at room temperature in an $N_2$ atmosphere for 24 hours. The volume of the solution was slowly reduced to a small amount on a rotary evaporator, and was added ether then precipitate formed in the solution. It was collected by filtration, washed with ether and recrystallized from methanol/ether. Yield: 28.0 mg ( 51.0%). $^1$H NMR (500 MHz, DMSO): δ 8.85 (d, J = 8.1 Hz, 2H), 8.75 (d, J = 5.3 Hz, 2H), 8.35 (td, J = 8.0, 1.2 Hz, 2H), 7.81 (d, J = 8.4 Hz, 4H), 7.75 (s, 2H), 7.59 (d, J = 8.3 Hz, 2H), 7.50 (s, 2H), 7.41 (s, 1H), 1.78 (s, 6H), 1.72 (s, 6H). Anal. Calcd for [$Cp^{biph}$Ir(bpy)Cl]Cl (692.7): C, 44.74; H, 3.75; N, 6.73. Found: C, 44.62; H, 3.71; N, 6.76.

**[$Cp^{biph}$Ir(bpy)Cl]$PF_6$** (**2**). $^1$H NMR (500 MHz, DMSO): δ 8.85 (d, J = 8.1 Hz, 2H), 8.75 (d, J = 5.3 Hz, 2H), 8.38 – 8.33 (m, 2H), 7.84 – 7.75 (m, 6H), 7.60 (d, J = 8.2 Hz, 2H), 7.51 (t, J = 7.6 Hz, 2H), 7.43 (d, J = 7.3 Hz, 1H), 1.79 (s, 6H), 1.73 (s, 6H). Anal. Calcd for [$Cp^{biph}$Ir(bpy)Cl]$PF_6$ (802.21): Anal.Caled: C, 47.62; N, 3.37; H, 4.24. Found: C, 45.86; N, 3.52; H, 3.80. [$X^-$] calcd for $PF_6$, 144.96; found, 145.00.

**[$Cp^{biph}$Ir(bpy)Cl]$BF_4$** (**3**). A solution of complex **1** (66.0 mg, 0.1 mmol) and $AgBF_4$ (20.1 mg, 0.1 mmol) in MeOH was stirred at room temperature in an $N_2$ atmosphere for 24 hours. The volume of the solution was slowly reduced to a small amount on a rotary evaporator, and was added ether then precipitate formed in the solution. It was collected by filtration, washed with ether and recrystallized from methanol/ether. Yield: 29.0 mg ( 41.0%). $^1$H NMR (500 MHz, DMSO): δ 8.85 (d, *J* = 8.1 Hz, 2H), 8.75 (d, *J* = 5.1 Hz, 2H), 8.36 (td, *J* = 7.9, 1.3 Hz, 2H), 7.85 – 7.81 (m, 4H), 7.79 – 7.76 (m, 2H), 7.60 (d, *J* = 8.3 Hz, 2H), 7.51 (t, *J* = 7.6 Hz, 2H), 7.43 (d, *J* = 7.4 Hz, 1H), 1.79 (s, 6H), 1.73 (s, 6H). Anal. Calcd for [$Cp^{biph}$Ir(bpy)Cl]$BF_4$ (744.05): C, 44.74; H, 3.75; N, 6.73. Found: C, 44.62; H, 3.71; N, 6.76. [$X^-$] calcd for $BF_4$, 87.00; found, 87.00.

**[$Cp^{biph}$Ir(bpy)Cl]$SbF_6$** (**4**). A solution of **[**$Cp^{biph}IrCl_2]_2$ (52.0 mg, 0.048 mmol), 2, 2′-bipyridine (16.0 mg, 0.10 mmol) and $NaSbF_6$ (25.1 mg, 0.097 mmol) in MeOH was stirred at room temperature in an $N_2$ atmosphere for 24 hours. The volume of the solution was slowly reduced to a small amount on a rotary evaporator, and was added n-hexane then precipitate formed in the solution. It was collected by filtration, washed with ether and recrystallized from methanol/ether. Yield: 35.2 mg ( 41.0%). $^1$H NMR (500 MHz, DMSO): δ 8.86 (s, 1H), 8.85 (s, 1H), 8.76 (d, *J* = 5.6 Hz, 2H), 8.36 (dd, *J* = 12.4, 4.6 Hz, 2H), 7.85 – 7.81 (m, 4H), 7.78 (s, 1H), 7.76 (s, 1H), 7.61 (s, 1H), 7.59 (s, 1H), 7.51 (t, *J* = 7.6 Hz, 2H), 7.43 (t, *J* = 7.4 Hz, 1H), 1.79 (s, 6H), 1.73 (s, 6H). Anal. Calcd for [$Cp^{biph}$Ir(bpy)Cl]$SbF_6$ (893.0): C, 44.74; H, 3.75; N, 6.73. Found: C, 44.62; H, 3.71; N, 6.76. [$X^-$] calcd for $SbF_6$, 234.89; found, 235.00.

**[Cp$^{biph}$Ir(bpy)Cl]$CF_3SO_3$** (**5**). A solution of [Cp$^{biph}$IrCl$_2$]$_2$ (53.7 mg, 0.05 mmol) and $AgCF_3SO_3$ (25.7 mg, 0.10 mmol) in MeOH was stirred at room temperature in an $N_2$ atmosphere for 24 hours, filtered. The volume of the solution was slowly reduced to a small amount on a rotary evaporator, 2, 2′-bipyridine (15.6 mg, 0.1 mmol) was added and after stirring at 328 K for 2.0 h. And was added ether then precipitate formed in the solution. It was collected by filtration, washed with ether and recrystallized from methanol/ether. Yield: 45.1 mg (58.2%). $^1$H NMR (500 MHz, DMSO): δ 8.85 (d, *J* = 8.1 Hz, 2H), 8.75 (d, *J* = 5.6 Hz, 2H), 8.38 – 8.33 (m, 2H), 7.86 – 7.80 (m, 4H), 7.79 – 7.75 (m, 2H), 7.60 (d, *J* = 8.3 Hz, 2H), 7.51 (t, *J* = 7.6 Hz, 2H), 7.42 (t, *J* = 7.4 Hz, 1H), 1.79 (s, 6H), 1.73 (s, 6H). Anal. Calcd for [Cp$^{biph}$Ir(bpy)Cl]$CF_3SO_3$ (806.32): C, 44.74; H, 3.75; N, 6.73. Found: C, 44.62; H, 3.71; N, 6.76. [X$^-$] calcd for $CF_3SO_3$, 148.95; found, 148.90.

**[Cp$^{biph}$Ir(bpy)Cl]$BPh_4$** (**6**). A solution of [Cp$^{biph}$IrCl$_2$]$_2$ (65.1 mg, 0.06 mmol) and 2, 2′-bipyridine (24.1 mg, 0.15 mmol) in MeOH was stirred at room temperature in an $N_2$ atmosphere for 24 hours. The volume of the solution was slowly reduced to a small amount on a rotary evaporator, $NH_4BPh_4$ (104.5 mg, 0.31 mmol) was added and after stirring at 277 K for 0.5 h, a precipitate formed in the solution. It was collected by filtration, washed with ether and recrystallized from methanol/ether. Yield: 54.5 mg ( 46.0%). A single crystal was obtained by slow evaporation of a methanol/diethyl ether solution at room temperature. $^1$H NMR (500 MHz, DMSO): δ 8.85 (d, *J* = 8.0 Hz, 3H), 8.76 (d, *J* = 5.8 Hz, 2H), 8.36 (t, *J* = 7.8 Hz, 3H), 7.82 (d, *J* = 8.4 Hz, 6H), 7.77 (d, *J* = 7.2 Hz, 3H), 7.74 (s, 5H), 7.62 (s, 12H), 7.51 (t, *J* = 7.7 Hz, 2H), 7.43 (d, *J* = 7.4 Hz, 1H), 1.79 (s, 6H), 1.73 (s, 6H).Anal. Calcd for [Cp$^{biph}$Ir(bpy)Cl]$BPh_4$ (976.48): C, 68.02; N, 2.78; H, 5.51. Found: C, 66.94; N, 3.04; H, 5.16. [X$^-$] calcd for $BPh_4$, 319.17; found, 319.20.

**[Cp$^{biph}$Ir(bpy)Cl]BArF** (**7**). A solution of complex **1** (20.9 mg, 0.030 mmol) and NaBAF (38.5 mg, 0.043 mmol) in MeOH was stirred at room temperature in an $N_2$ atmosphere for 24 hours. The volume of the solution was slowly reduced to a small amount on a rotary evaporator, and was added n-hexane then precipitate formed in the solution. It was collected by filtration, washed with ether and recrystallized from methanol/ether.Yield: 22.3 mg (50%). $^1$H NMR (500 MHz, DMSO): δ 8.85 (d, *J* = 8.1 Hz, 2H), 8.75 (d, *J* = 5.4 Hz, 2H), 8.35 (dd, *J* = 16.8, 9.0 Hz, 2H), 7.86 – 7.79 (m, 6H), 7.79 – 7.71 (m, 4H), 7.66 – 7.56 (m, 10H), 7.51 (t, *J* = 7.7 Hz, 2H), 7.42 (t, *J* = 7.3 Hz, 1H), 1.79 (s, 6H), 1.72 (s, 6H). Anal. Calcd for [Cp$^{biph}$Ir(bpy)Cl]BArF (1520.46): C, 49.77; H, 2.72; N, 1.84. Found: C, 50.14; H, 3.49; N, 1.80. [X$^-$] calcd for BArF, 863.07; found, 862.80.

**Methods and Instrumentation.** X-ray Diffraction data were collected at 298 K on a Bruker Smart CCD area detector with graphite-monochromated Mo K$^\alpha$ radiation (λ = 0.71073 Å). Absorption corrections were applied using ABSPACK. The crystals were mounted in oil and held at 100 K with the Oxford Chrysostom Cobra. The structures were solved by direct methods using SHELXS (TREF) with additional light atoms found by Fourier methods. Complexes were refined against $F^2$ using SHELXL, and hydrogen atoms were added at calculated positions and refined riding on their parent atoms.

X-ray crystallographic data for complex **6** is available as **Tables S1-S2.** CCDC numbers of **6** is 1828780. These data can be obtained free of charge from the Cambridge Crystallographic Data Centre via www.ccdc.cam.ac.uk/data_request/cif.

**NMR Spectroscopy.** $^1$H NMR spectra were captured in 5 mm NMR tubes at 298 K on Bruker DPX 500 ($^1$H = 500.13 MHz) spectrometers. $^1$HNMR chemical shifts were internally referenced to

$(CHD_2)(CD_3)SO$ (2.50 ppm) for DMSO-$d_6$, $CHCl_3$ (7.26 ppm) for chloroform-$d_1$, $CHD_2OD$ (3.33 ppm) for methanol-$d_4$. All data processing was done using XWIN-NMR version 3.6 (Bruker UK Ltd.).

**UV-Vis Spectroscopy.** The properties of the compounds were determined by TU-1901 UV spectrophotometer. Quartz cuvette path length is 1 cm (3 ml). Spectra were processed using UVWinlab software. If there is no particular requirement, the experiment will be carried out at room temperature.

**Hydrolysis Studies.** Solutions of complexes **1-7** with final concentrations of 50 μM in 10% MeOH/90% $H_2O$ (v/v) were prepared by dissolution of the complex in MeOH followed by rapid dilution with $H_2O$. UV-vis spectra of these solutions were recorded at 298 K after various time intervals. **Fig 2b** and **2c** in the article represent the difference spectra between the immersion times of 0.5 h, 2 h, 3 h, 5h, 6h, 7 h, 8 h and 1 min of the normalized UV-vis spectra.

**Reaction with NADH.** NADH (3.5 mol equiv) was added to an NMR tube containing a 0.8 mM solution of complex **5** in 50% $CD_3OD$/50% $D_2O$ (v/v), $^1H$ NMR spectra of these solutions were recorded at 298 K after different time intervals. The response of complexes **1-7** (ca. 1 μM) with NADH (ca. 90 μM) in 10% MeOH/90% $H_2O$ (v/v) was monitored by UV-Vis at 298 K after various time intervals.

**Cell Culture.** A549 human lung cancer cells were obtained from Shanghai Institute of Biochemistry and Cell Biology (SIBCB) and were grown in Dubelco's Modified Eagle Medium (DMEM). All media were supplemented with 10% fetal bovine serum, and 1 % penicillin-streptomycin solution. All cells were grown at 310 K in a humidified incubator under a 5 % $CO_2$ atmosphere.

**Viability assay (MTT assay).** After plating 5000 A549 human lung cancer cells per well in 96-well plates, the cells were preincubated in drug-free media at 310 K for 24 h before adding different concentrations of the compounds to be tested. In order to prepare the stock solution of the drug, the solid complex was dissolved in DMSO. This stock was further diluted using cell culture medium until working concentrations were achieved. The drug exposure period was 24 h. Subsequently, 15 μl of 5 mg $ml^{-1}$ MTT solution was added to form a purple formazan. Afterwards, 100 μl of dimethyl sulfoxide (DMSO) was transferred into each well to dissolve the purple formazan, and results were measured using a microplate reader (DNM-9606, Perlong Medical, Beijing, China) at an absorbance of 570 nm. Each well was triplicated and each experiment repeated at least three times. $IC_{50}$ values quoted are mean ± SEM.

**Cell Cycle Analysis.** A549 human lung cancer cells at $1.5 \times 10^6$ per well were seeded in a six-well plate. Cells were preincubated in drug-free media at 310 K for 24 h, after which drugs were added at concentrations of $0.25 \times IC_{50}$, $0.5 \times IC_{50}$ and $1.0 \times IC_{50}$. After 24 h of drug exposure, supernatants were removed by suction and cells were washed with PBS. Finally, cells were harvested using trypsin-EDTA and fixed for 24 h using cold 70 % ethanol. DNA staining was achieved by resuspending the cell pellets in PBS containing propidium iodide (PI) and RNAse. Cell pellets were washed and resuspended in PBS before being analyzed in a flow cytometer (ACEA NovoCyte, Hangzhou, China) using excitation of DNA-bound PI at 488 nm, with emission at 585 nm. Data were processed using NovoExpress™ software. The cell cycle distribution is shown as the percentage of cells containing $G_0/G_1$, S and $G_2$/M DNA as identified by propidium iodide staining.

**Induction of Apoptosis.** Flow cytometry analysis of apoptotic populations of A549 human

lung cancer cells caused by exposure to iridium complexes was carried out using the Annexin V-FITC Apoptosis Detection Kit (Beyotime Institute of Biotechnology, China) according to the supplier's instructions. Briefly, A549 human lung cancer cells ($1.5 \times 10^6$/2 ml per well) were seeded in a six-well plate. Cells were preincubated in drug-free media at 310 K for 24 h, after which drugs were added at concentrations of $0.5 \times IC_{50}$, $1 \times IC_{50}$ and $2 \times IC_{50}$. After 24 h of drug exposure, cells were collected, washed once with PBS, and resuspended in 195 µl of annexin V-FITC binding buffer which was then added to 5 µl of annexin V-FITC and 10 µl of PI, and then incubated at room temperature in the dark for 15 min. Subsequently, the buffer placed in an ice bath in the dark. The samples were analyzed by a flow cytometer (ACEA NovoCyte, Hangzhou, China).

**ROS Determination.** Flow cytometry analysis of ROS generation in A549 human lung cancer cells caused by exposure to iridium complexes was carried out using the Reactive Oxygen Species Assay Kit (Beyotime Institute of Biotechnology, Shanghai, China) according to the supplier's instructions. Briefly, $1.5 \times 10^6$ cells per well were seeded in a six-well plate. Cells were preincubated in drug-free media at 310 K for 24 h in a 5 % $CO_2$ humidified atmosphere, and then drugs were added at concentrations of $0.25 \times IC_{50}$ and $0.5 \times IC_{50}$. After 24 h of drug exposure, cells were washed twice with PBS and then incubated with the DCFH-DA probe (10 µM) at 37 °C for 30 min, and then washed triple immediately with PBS. The fluorescence intensity was analyzed by flow cytometry (ACEA NovoCyte, Hangzhou, China). Data were processed using NovoExpress™ software. At all times, samples were kept under dark conditions to avoid light-induced ROS production.

**Mitochondrial Membrane Assay**. Analysis of the changes of mitochondrial potential in cells after exposure to iridium complexes was carried out using the Mitochondrial membrane potential assay kit with JC-1 (Beyotime Institute of Biotechnology, Shanghai, China) according to the manufacturer's instructions. Briefly, $1.5 \times 10^6$ A549 cancer cells were seeded in six-well plates left to incubate for 24 h in drug-free medium at 310 K in a humidified atmosphere. Drug solutions, at concentrations of $0.25 \times IC_{50}$, $0.5 \times IC_{50}$, $1.0 \times IC_{50}$ and $2.0 \times IC_{50}$ of complexes **5** and **6** against A549 cancer cells, were added in triplicate, and the cells were left to incubate for a further 24 h under similar conditions. Supernatants were removed by suction, and each well was washed with PBS before detaching the cells using trypsin-EDTA. Staining of the samples was done in flow cytometry tubes protected from light, incubating for 30 min at ambient temperature. The samples were immediately analyzed by a flow cytometer (ACEA NovoCyte, Hangzhou, China). For positive controls, the cells were exposed to carbonyl cyanide 3-chlorophenylhydrazone, CCCP (5 µM), for 20 min. Data were processed using NovoExpress™ software.

1. Z. Liu, A. Habtemariam, A. M. Pizarro, S. A. Fletcher, A. Kisova, O. Vrana, L. Salassa, P. C. Bruijnincx, G. J. Clarkson, V. Brabec and P. J. Sadler, *J. Med. Chem.*, 2011, **54**, 3011-3026.

**Table S1.** Selected Bond Lengths (Å) and Angles (deg) for Complexes **2** and **6**.

| | **6** | 2 |
|---|---|---|
| Ir-$N_1$ | 2.088 (4) | 2.086 (4) |
| Ir-$N_2$ | 2.101 (3) | 2.091 (5) |
| Ir-C(cyclopentadienyl) | 2.157 (4) | 2.151 (5) |
| | 2.167 (4) | 2.155 (5) |
| | 2.179 (4) | 2.161 (5) |
| | 2.185 (4) | 2.172 (5) |
| | 2.189 (5) | 2.184 (5) |
| Ir-C (centroid) | 1.7979 | 1.787 |
| Ir-Cl | 2.3966 (13) | 2.3840 (14) |
| $N_1$-Ir-$N_2$ | 76.67 (14) | 76.76 (16) |
| $N_1$-Ir-Cl | 84.31 (11) | 84.84 (11) |
| $N_2$-Ir-Cl | 83.36 (11) | 86.20 (14) |

**Table S2.** Crystallographic Data for $[Cp^{biph}Ir(bpy)Cl]BPh_4$ (**6**).

| | **6** |
|---|---|
| formula | $C_{55}H_{49}BClIrN_2$ |
| MW | 976.42 |
| cryst | yellow block |
| Cryst size(mm) | 0.43 × 0.28 × 0.22 |
| λ (Å) | 0.71073 |
| temp(K) | 298 |
| cryst syst | Monoclinic |
| space group | P2(1)/n |
| a (Å) | 20.4266(18) |
| b (Å) | 9.3782(7) |
| c (Å) | 24.537(2) |
| α (°) | 90 |
| β (°) | 108.456(2) |
| γ (°) | 90 |
| vol($Å^3$) | 4458.7(6) |
| Z | 4 |
| R($Fo^2$) | 0.0362 |
| Rw($Fo^2$) | 0.0812 |
| GOF | 1.037 |

**Table S3.** Hydrolysis data for complexes **1-7** at 298 K monitored by UV-Vis.

| Complex | k ( $min^{-1}$ ) | $t_{1/2}$ ( min ) |
|---|---|---|
| **1** | 0.050 | 13.7 |
| **2** | 0.009 | 74.2 |
| **3** | 0.031 | 22.3 |
| **4** | 0.011 | 62.2 |
| **5** | 0.036 | 19.0 |
| **6** | 0.003 | 182.8 |
| **7** | 0.004 | 147.4 |

**Table S4**. Cell cycle analysis carried out by flow cytometry using PI staining after exposing A549 cells to complex **5**.

| Complex | Ir concentration | Population (%) | | | |
|---|---|---|---|---|---|
| | | $G_0/G_1$ phase | S phase | $G_2$/M phase | Sub-$G_1$ |
| **5** | 0.25 × $IC_{50}$ | 56.90 ± 1.3 | 33.00 ± 0.2 | 12.31 ± 0.9 | 0.13 ± 0.01 |
| **5** | 0.5 × $IC_{50}$ | 57.27 ± 0.4 | 32.91 ± 1.7 | 11.96 ± 2.0 | 0.36 ± 0.02 |
| **5** | 1.0 × $IC_{50}$ | 43.57 ± 0.1 | 37.69 ± 2.1 | 18.31 ± 0.7 | 0.58 ± 0.12 |
| **control** | | 58.88 ± 1.4 | 30.86 ± 1.2 | 11.39 ± 1.1 | 0.06 ± 0.03 |

**Table S5**. Cell cycle analysis carried out by flow cytometry using PI staining after exposing A549 cells to complex **6**.

| Complex | Ir concentration | Population (%) | | |
|---|---|---|---|---|
| | | $G_0/G_1$ phase | S phase | $G_2$/M phase |
| **6** | 0.25 × $IC_{50}$ | 48.01 ± 0.3 | 29.76 ± 0.4 | 21.84 ± 1.3 |
| **6** | 0.5 × $IC_{50}$ | 48.11 ± 0.1 | 30.48 ± 1.6 | 22.43 ± 2.1 |
| **6** | 1.0 × $IC_{50}$ | 46.74 ± 2.6 | 31.75 ± 1.1 | 21.63 ± 1.0 |
| **control** | | 47.55 ± 0.1 | 28.14 ± 0.1 | 22.65 ± 0.4 |

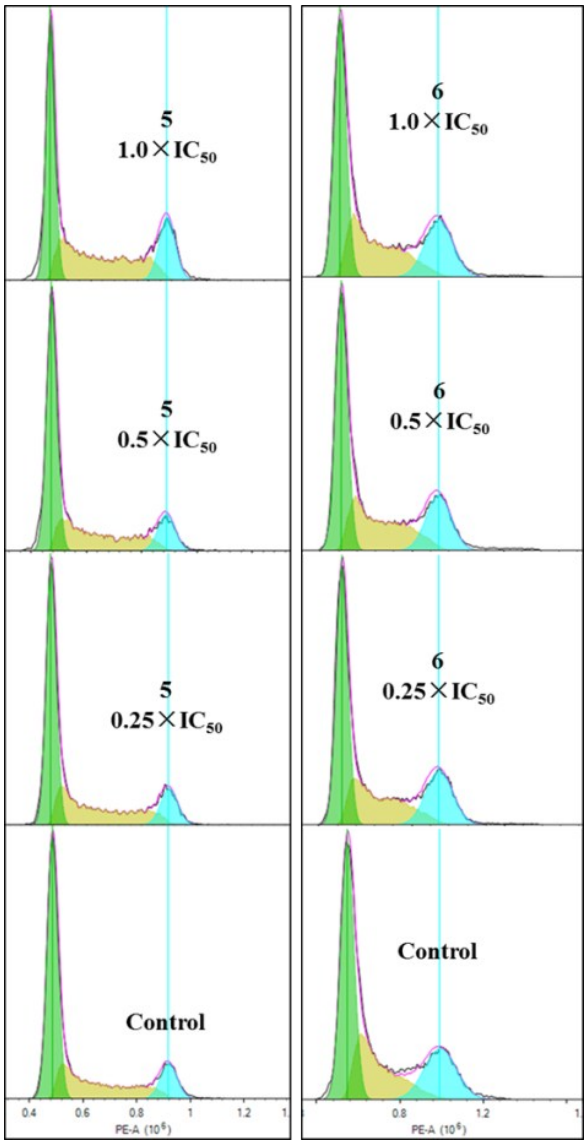


**Figure S1**: Flow cytometry data for cell cycle distribution of A549 cancer cells exposed to complexes **5** and **6** for 24 h. Concentrations used were 0.25, 0.5 and 1 equipotent concentrations of $IC_{50}$. Cell staining for flow cytometry was carried out using PI/RNase.

**Table S6**. Flow cytometry analysis to determine the percentages of apoptotic cells, using Annexin V-FITC vs PI staining, after exposing A549 cells to complex **5**.

| Complex | Ir concentration | Population（%） | | | |
|---|---|---|---|---|---|
| | | Viable | Early apoptosis | Late apoptosis | Non-viable |
| **5** | 0.5 × $IC_{50}$ | 94.92 ± 0.1 | 1.34 ± 0.8 | 2.43 ± 0.1 | 1.32 ± 0.8 |
| **5** | 1 × $IC_{50}$ | 87.73 ± 4.4 | 2.82 ± 1.0 | 7.06 ± 2.6 | 2.4 ± 0.8 |
| **5** | 2 × $IC_{50}$ | 49.0 ± 5.6 | 25.65 ± 2.7 | 22.47 ± 2.4 | 2.87 ± 0.5 |
| **control** | | 95.77 ± 0.7 | 0.36 ± 0.2 | 3.21 ± 0.1 | 0.66 ± 0.4 |

**Table S7**. Flow cytometry analysis to determine the percentages of apoptotic cells, using Annexin V-FITC vs PI staining, after exposing A549 cells to complex **6**.

| Complex | Ir concentration | Population（%） | | | |
|---|---|---|---|---|---|
| | | Viable | Early apoptosis | Late apoptosis | Non-viable |
| **6** | 0.5 × $IC_{50}$ | 79.04 ± 3.3 | 10.63 ± 2.8 | 8.05 ± 0.1 | 2.29 ± 0.5 |
| **6** | 1 × $IC_{50}$ | 78.19 ± 0.9 | 9.46 ± 1.1 | 9.60 ±0.1 | 2.76 ± 0.3 |
| **6** | 2 × $IC_{50}$ | 80.25 ± 2.1 | 6.21 ± 0.1 | 8.73 ± 0.1 | 4.82 ± 1.9 |
| **control** | | 88.07 ± 0.7 | 5.46 ± 0.2 | 5.64 ± 0.1 | 0.10 ± 0.4 |

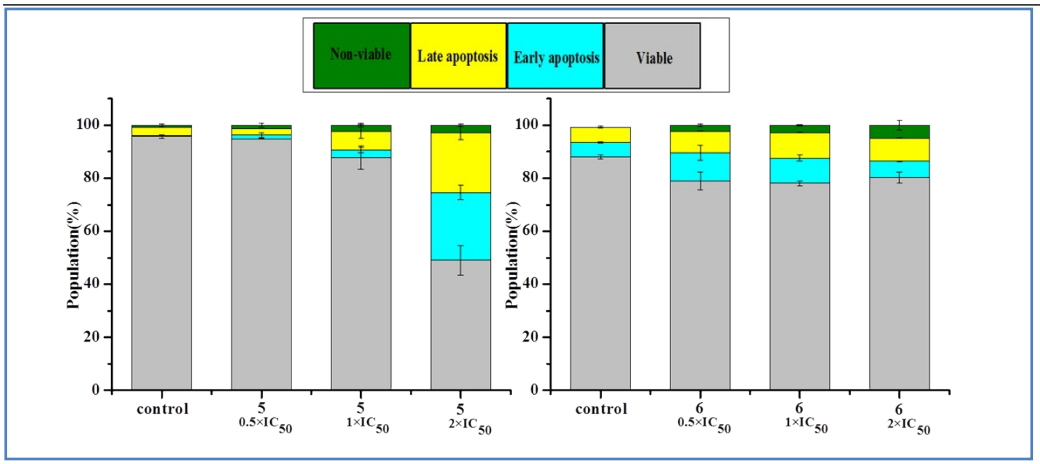


**Figure S2**. Apoptosis analysis of populations for cells in four stages treated by complexes **5** and **6**. Data are quoted as mean ± SD of three replicates.

**Table S8**. ROS induction in A549 cancer cells treated with complex **5**.

| Complex | Ir concentration | Fluorescence Intensity |
|---|---|---|
| **5** | 0.25 × $IC_{50}$ | 1, 249, 683 |
| | 0.5 × $IC_{50}$ | 1, 322, 695 |
| **Untreated cells (Negative Control)** | | 789, 298 |
| **CCCP treated cells (Positive Control)** | | 2, 333, 259 |

**Table S9**. ROS induction in A549 cancer cells treated with complex **6**.

| Complex | Ir concentration | Fluorescence Intensity |
|---|---|---|
| **6** | 0.25 × $IC_{50}$ | 574, 111.5 |
| | 0.5 × $IC_{50}$ | 603, 922.5 |
| **Untreated cells (Negative Control)** | | 550, 671 |
| **CCCP treated cells (Positive Control)** | | 2, 333, 259 |

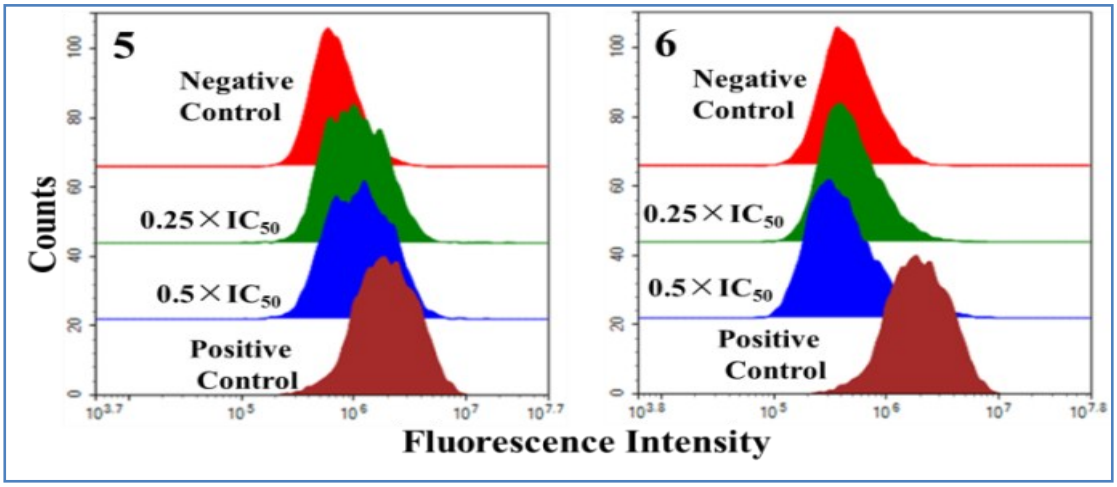


**Figure S3**. Changes in mitochondrial membrane potential of A549 cancer cells induced by complexes **5** and **6**.

**Table S10**. The mitochondrial membrane polarization of A549 cells induced by complex **5**.

| | | Population (%) | |
|---|---|---|---|
| **Complex** | **Ir concentration** | **JC-1 Aggregates** | **JC-1 Monomers** |
| **5** | 0.25 × $IC_{50}$ | 79.6 ± 0.8 | 19.9 ± 0.7 |
| | 0.5 × $IC_{50}$ | 67.7 ± 1.1 | 31.6 ± 1.1 |
| | 1.0 × $IC_{50}$ | 45.1 ± 1.4 | 54.3 ± 1.4 |
| | 2.0 × $IC_{50}$ | 10.1 ± 0.3 | 88.8 ± 0.3 |
| **Negative Control** | | 84.4 ± 3.1 | 14.8 ± 3.1 |
| **Positive Control** | | 18.5 ± 1.6 | 79.4 ± 1.0 |

**Table S11**. The mitochondrial membrane polarization of A549 cancer cells induced by complex **6**.

| | | Population (%) | |
|---|---|---|---|
| **Complex** | **Ir concentration** | **JC-1 Aggregates** | **JC-1 Monomers** |
| **6** | 0.25 × $IC_{50}$ | 80.5 ± 0.1 | 17.9 ± 0.1 |
| | 0.5 × $IC_{50}$ | 74.4 ± 2.1 | 23.1 ± 2.8 |
| | 1.0 × $IC_{50}$ | 69.6 ± 1.6 | 27.8 ± 1.4 |
| | 2.0 × $IC_{50}$ | 57.0 ± 1.5 | 38.2 ± 1.6 |
| **Negative Control** | | 81.5 ± 2.5 | 16.6 ± 2.7 |
| **Positive Control** | | 18.5 ± 2.0 | 79.4 ± 2.0 |

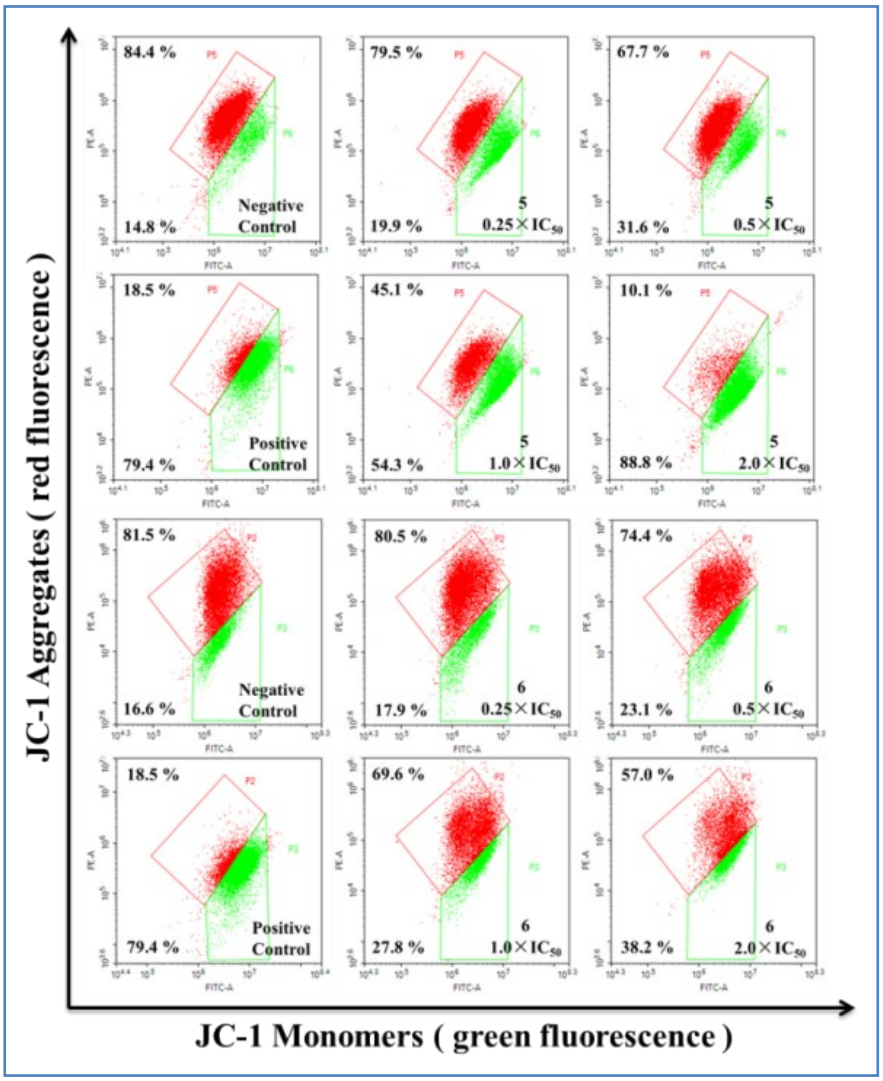


**Figure S4**. Changes in mitochondrial membrane potential of A549 cancer cells induced by complexes **5** and **6**.

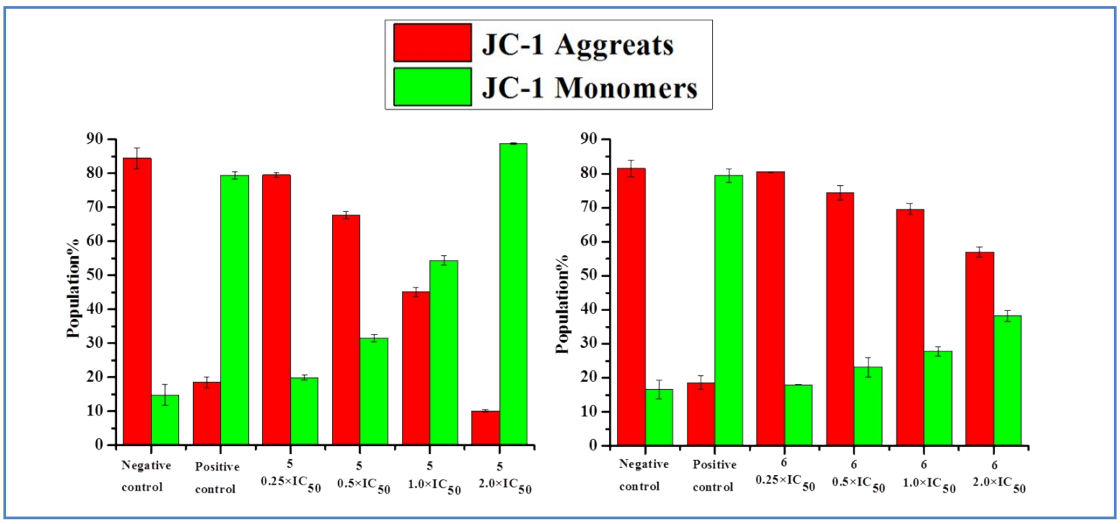


**Figure S5**. Changes in mitochondrial membrane potential of A549 cancer cells induced by complexes **5** and **6**. Populations of cells that exhibit a reduction in the mitochondrial membrane potential. Data are quoted as mean ± SD of three replicates.

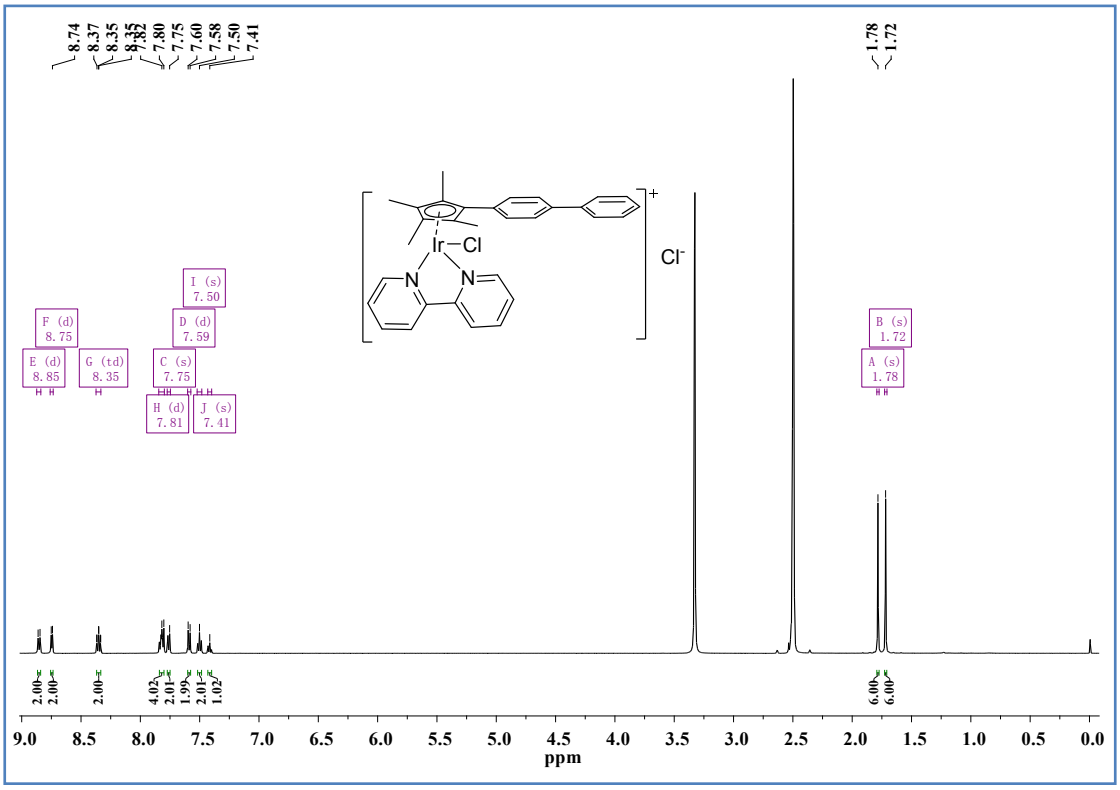


**Figure S6**: The $^{1}$H NMR (500.13 MHz, DMSO-d$_6$) peak integrals of complex **1**.

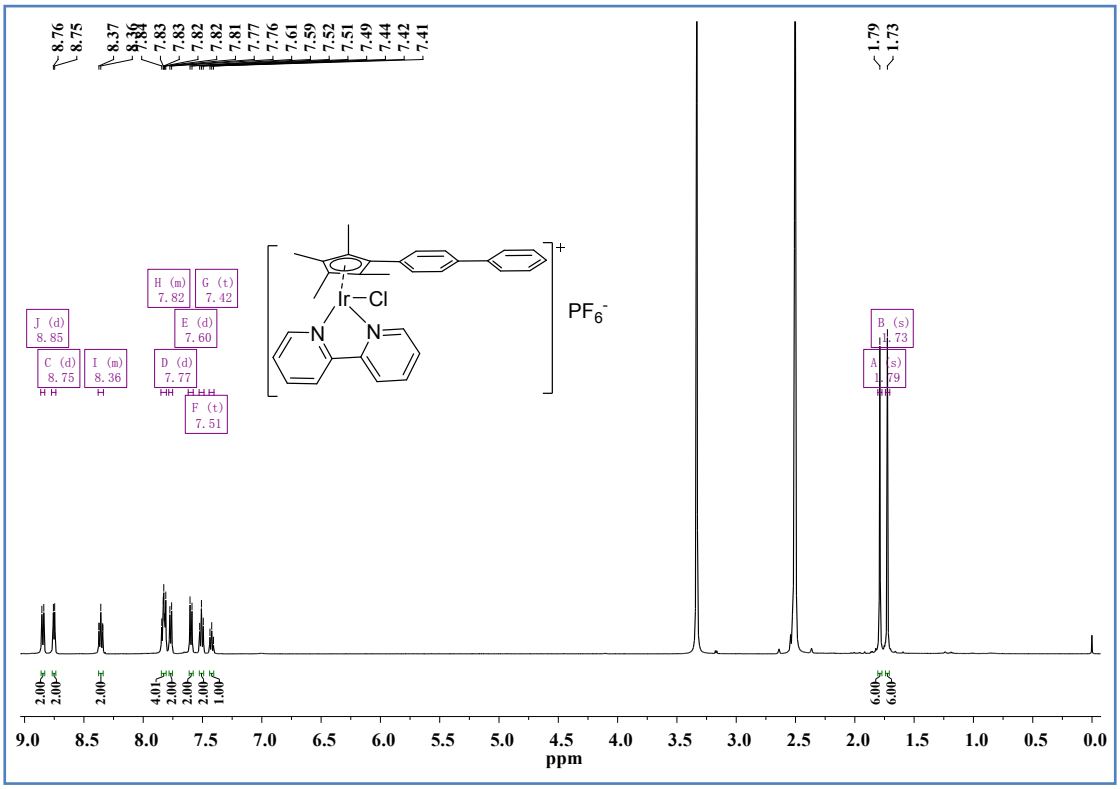


**Figure S7**: The $^{1}$H NMR (500.13 MHz, DMSO-d$_6$) peak integrals of complex **2**.

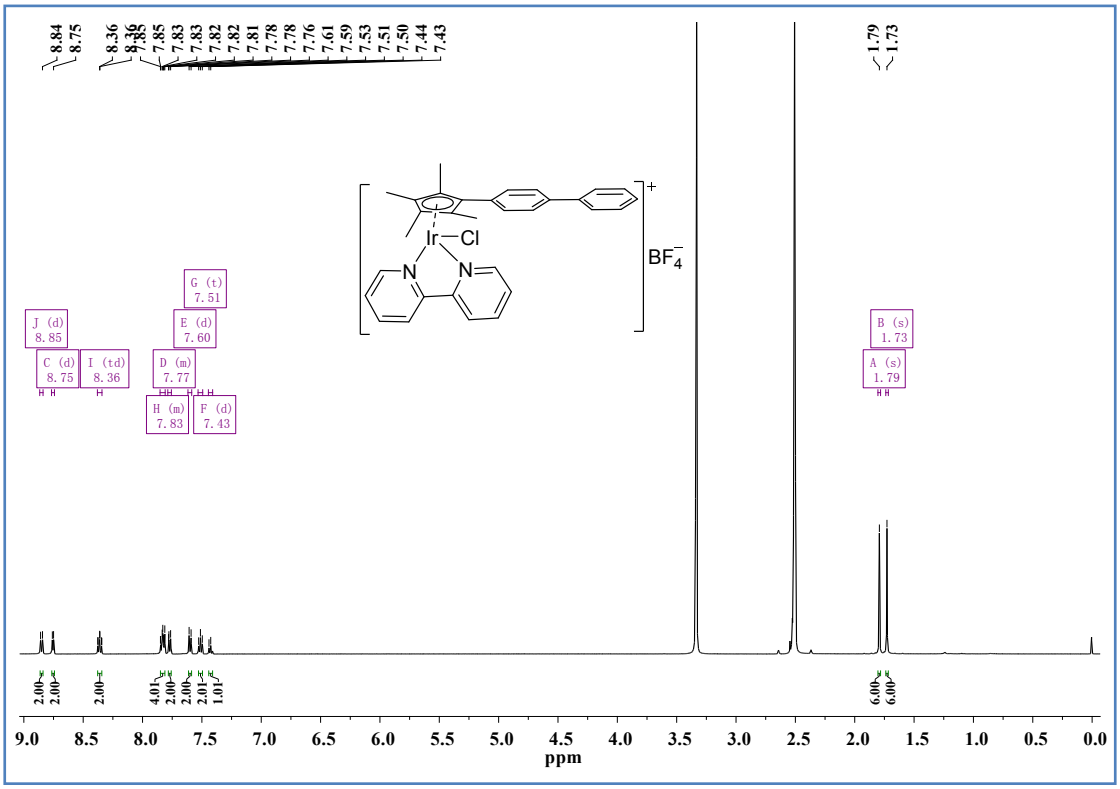


**Figure S8**: The $^{1}$H NMR (500.13 MHz, DMSO-d$_6$) peak integrals of complex **3**.

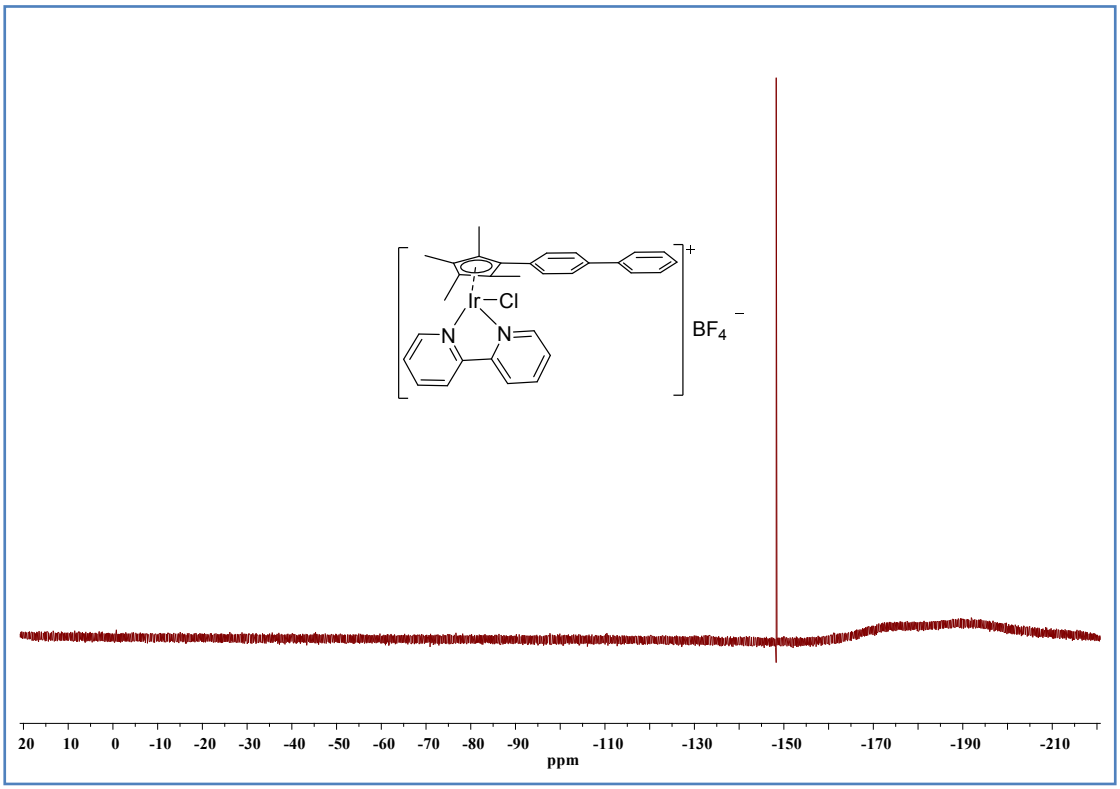


**Figure S9**: The $^{19}$F NMR (500.13 MHz, DMSO-d$_6$) peak integrals of complex **3**.

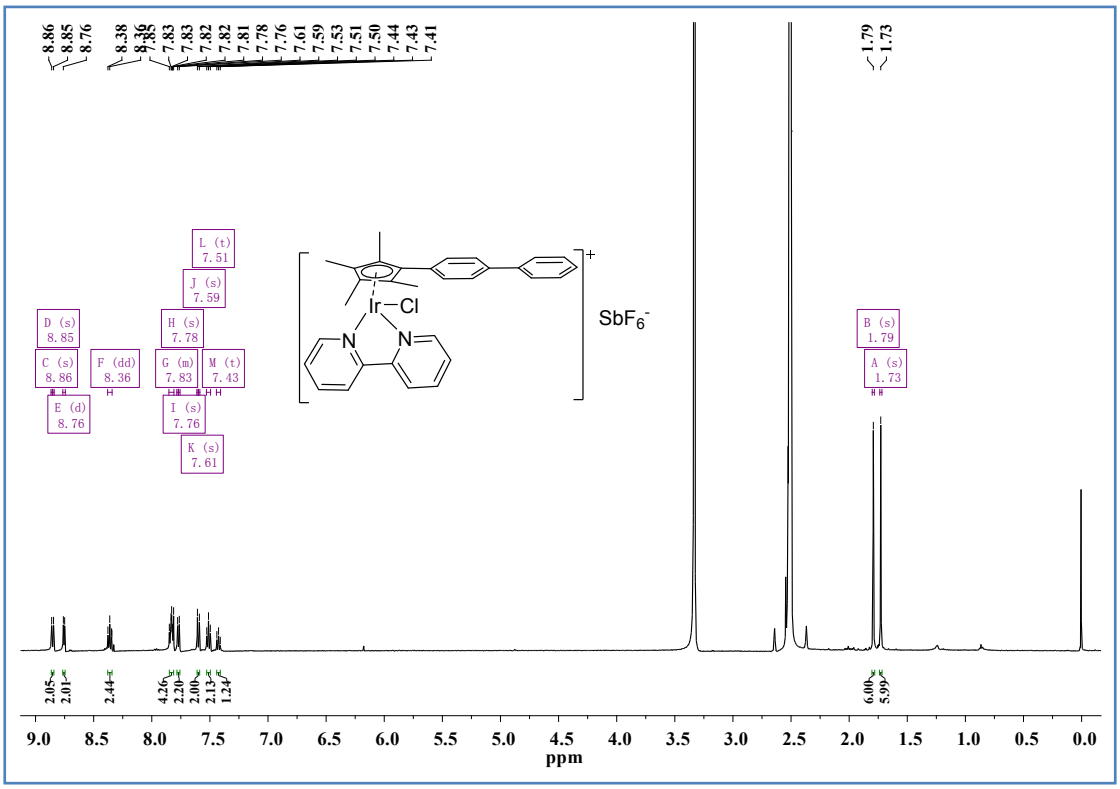


**Figure S10**: The $^{1}$H NMR (500.13 MHz, DMSO-d$_6$) peak integrals of complex **4**.

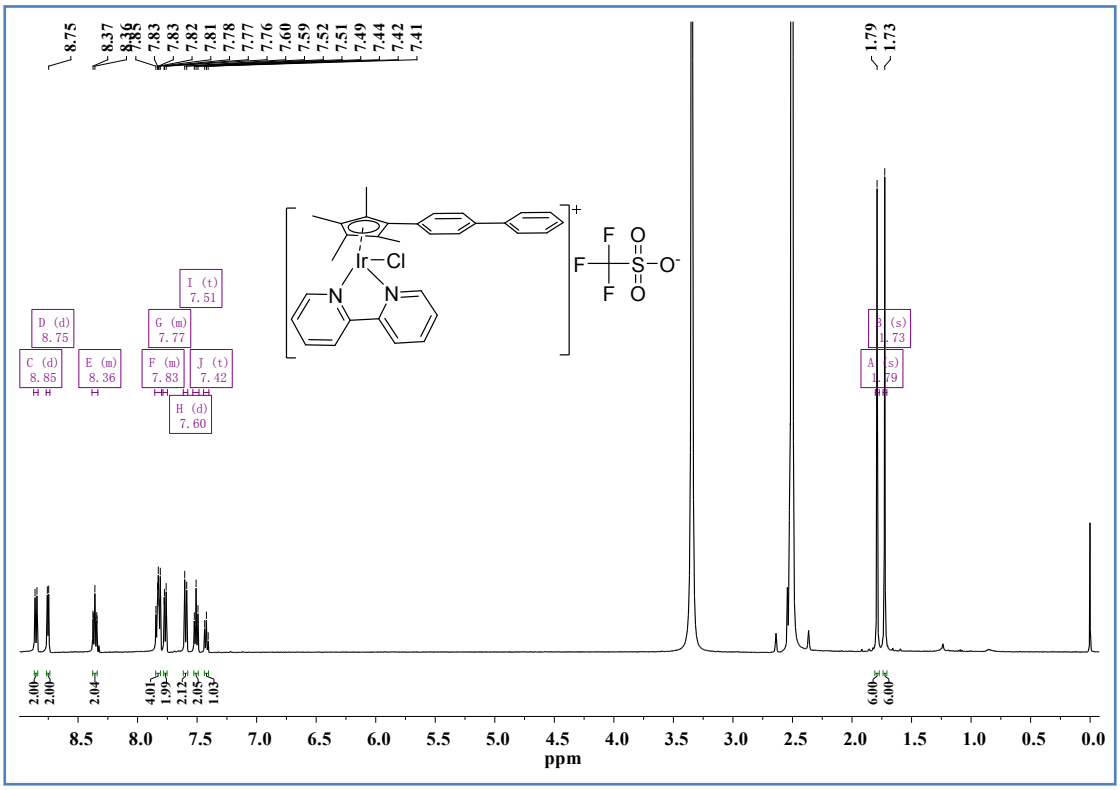


**Figure S11**: The $^{1}$H NMR (500.13 MHz, DMSO-d$_6$) peak integrals of complex **5**.

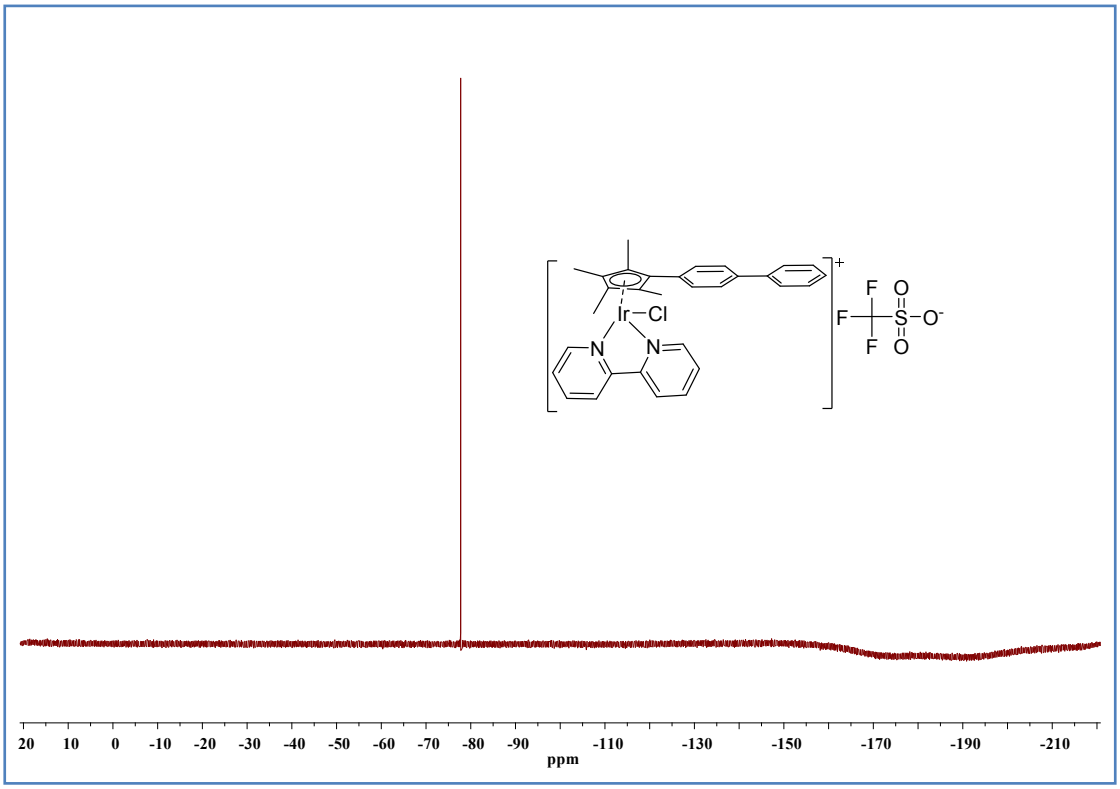


**Figure S12**: The $^{19}F$ NMR (500.13 MHz, DMSO-$d_6$) peak integrals of complex **5**.

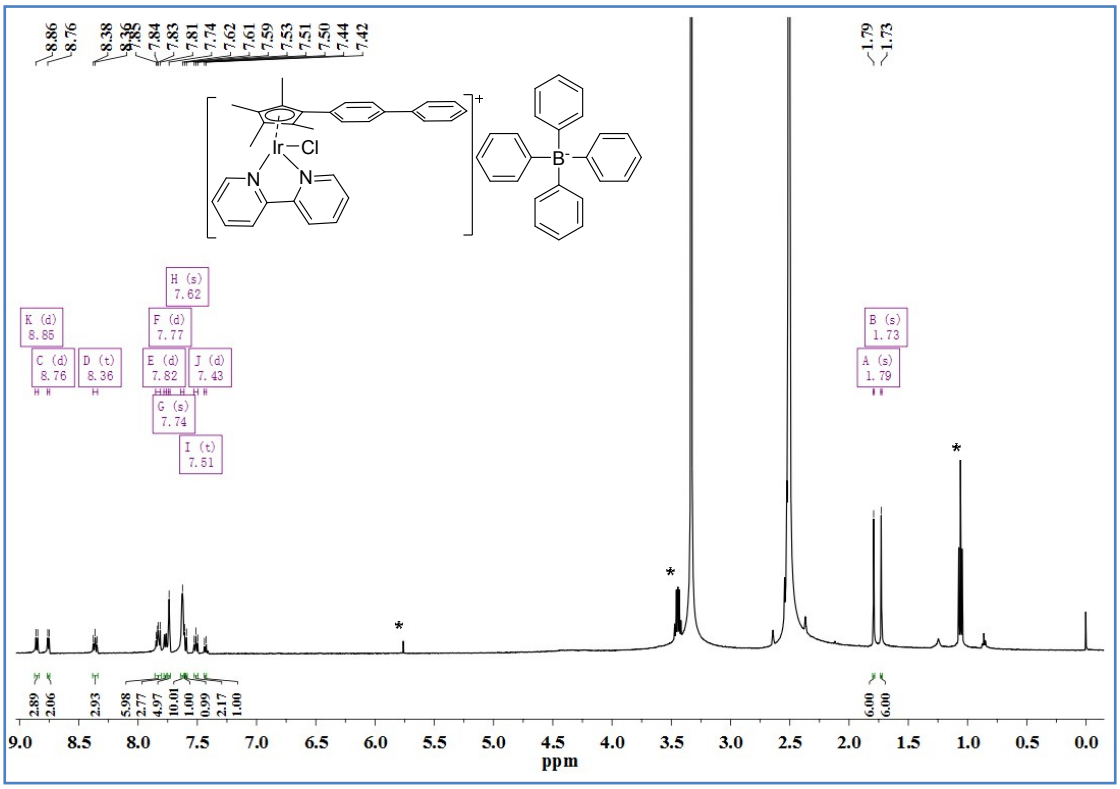


**Figure S13**: The $^{1}H$ NMR (500.13 MHz, DMSO-$d_6$) peak integrals of complex **6**. * $CH_2Cl_2$, ethanol

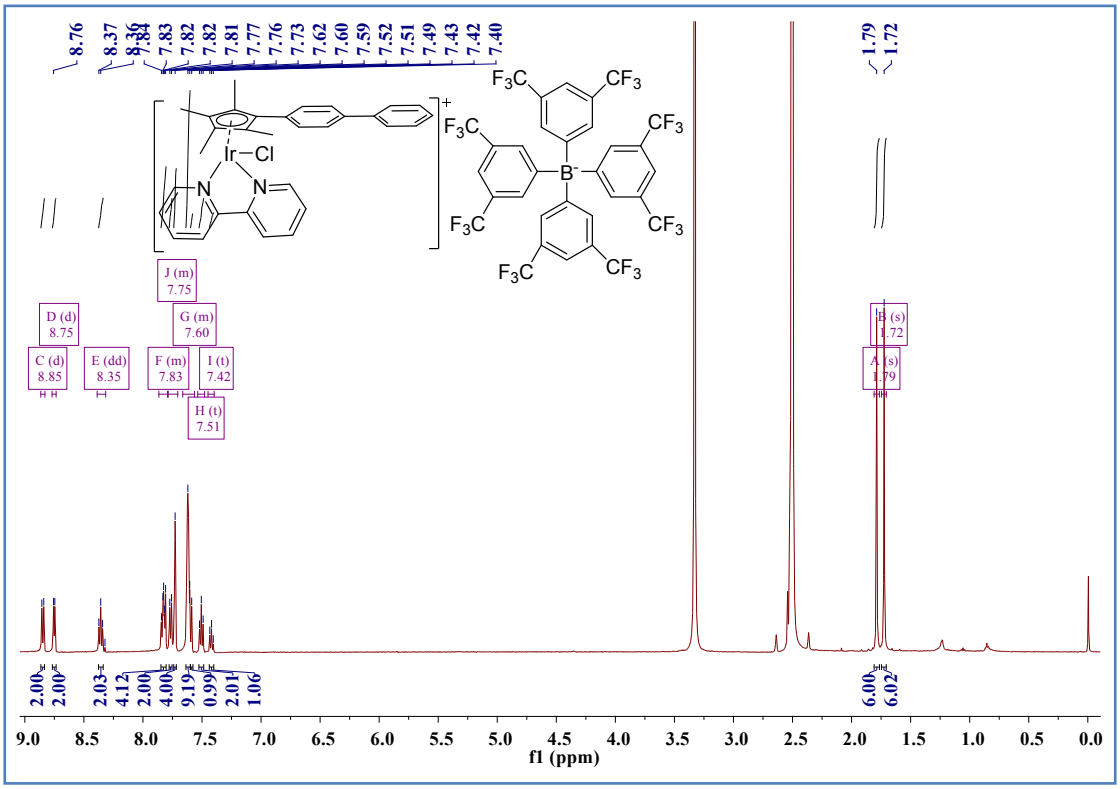


**Figure S14**: The $^{1}$H NMR (500.13 MHz, DMSO-d$_6$) peak integrals of complex **7**.

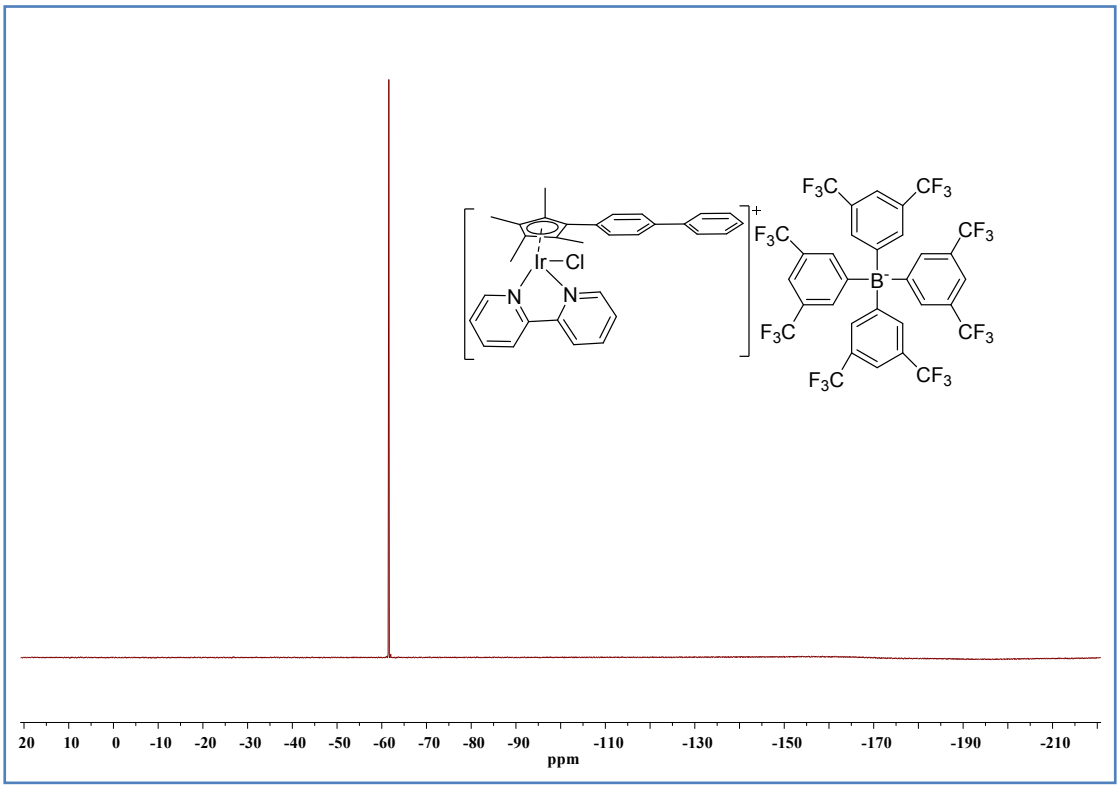


**Figure S15**: The $^{19}$F NMR (500.13 MHz, DMSO-d$_6$) peak integrals of complex **7**.

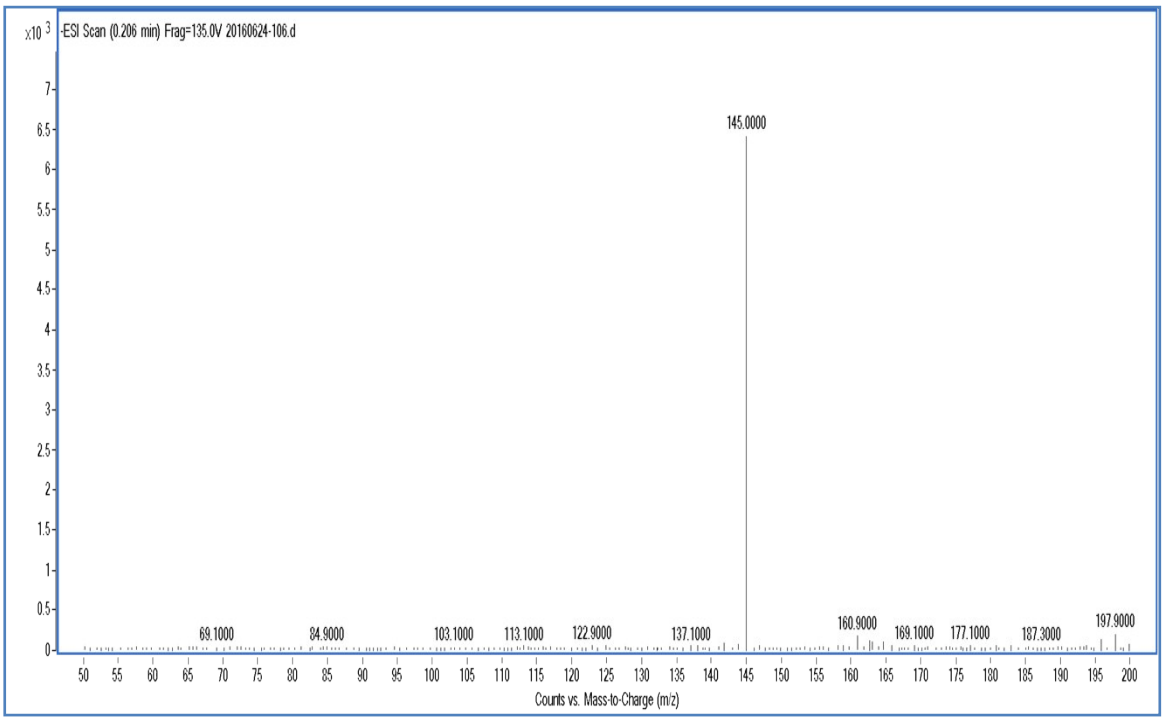


**Figure S16**: The anionic mass spectrum of complex **2** ($PF_6^-$).

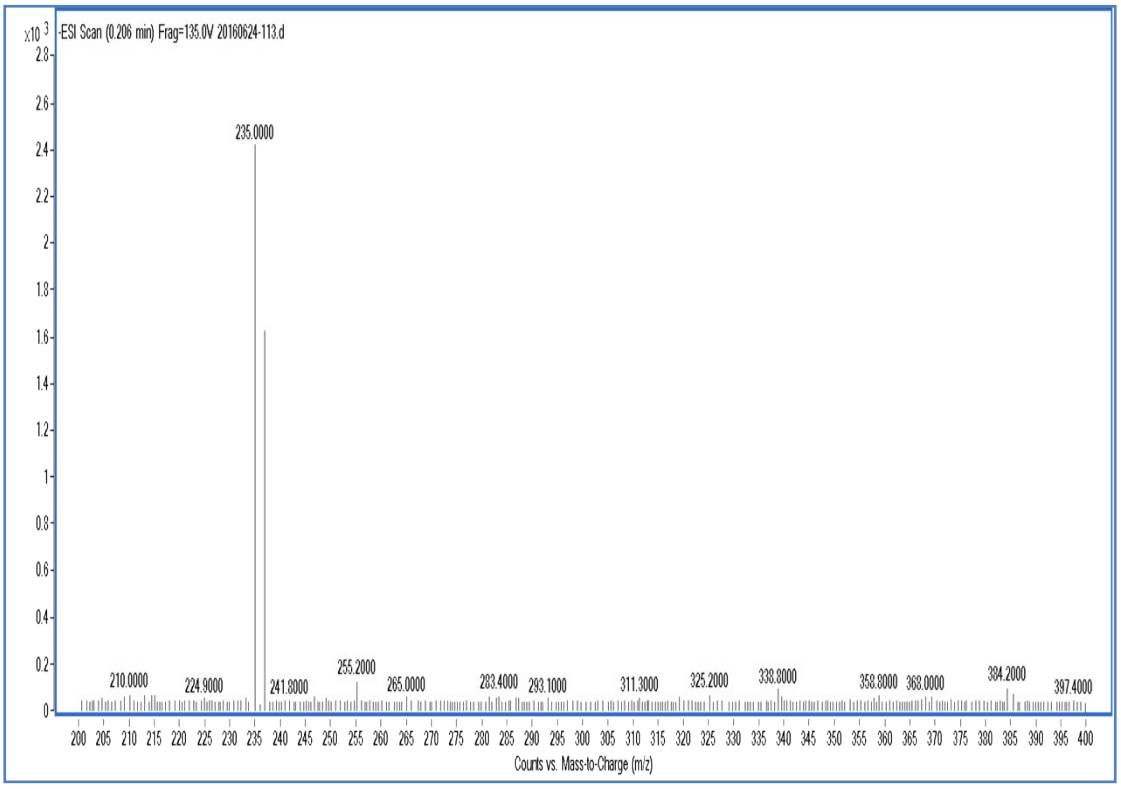


**Figure S17**: The anionic mass spectrum of complex **4** ($SbF_6^-$).

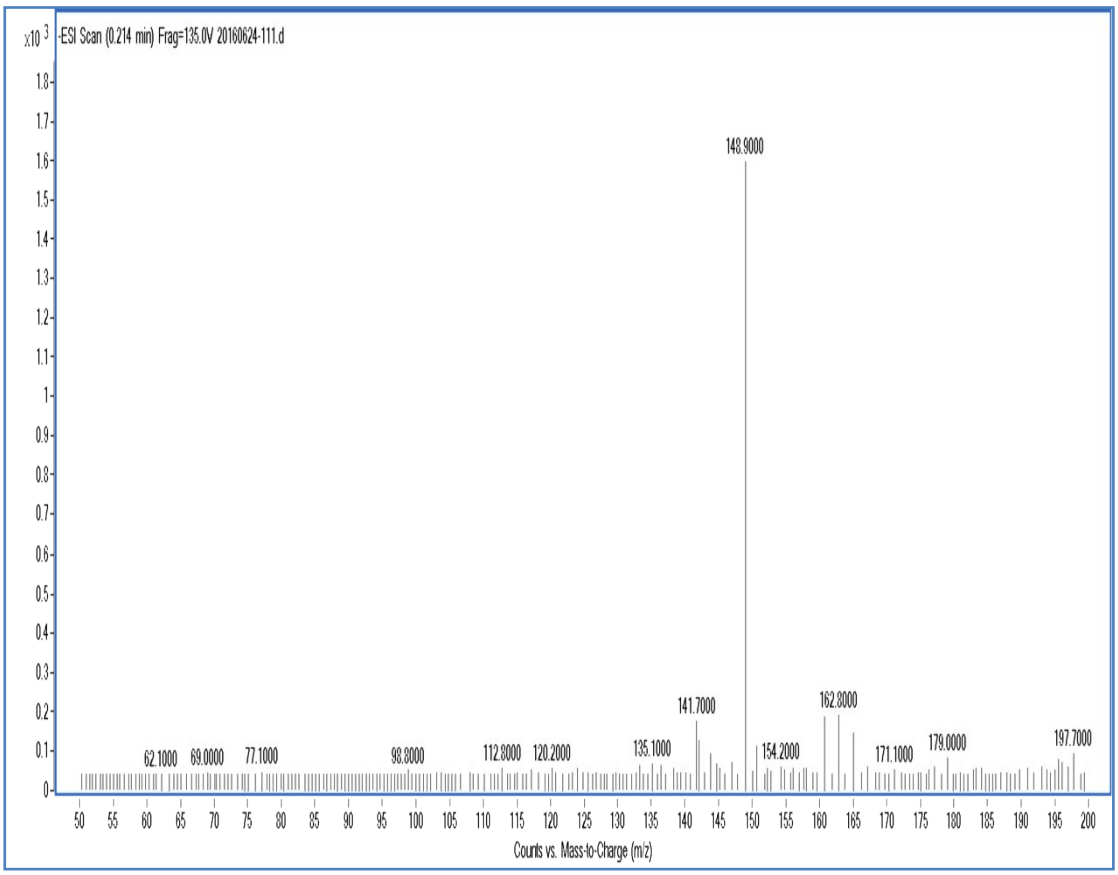


**Figure S18**: The anionic mass spectrum of complex **5** ($CF_3SO_3^-$).

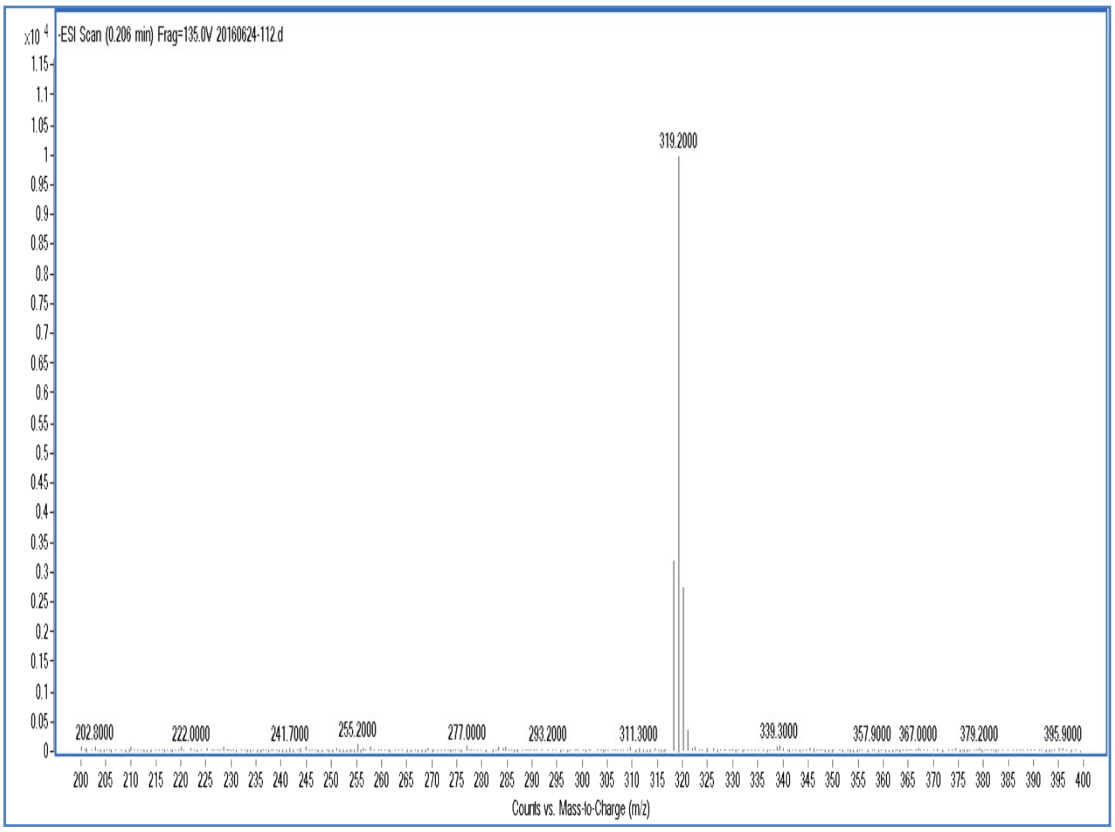


**Figure S19**: The anionic mass spectrum of complex **6** ($BPh_4^-$).

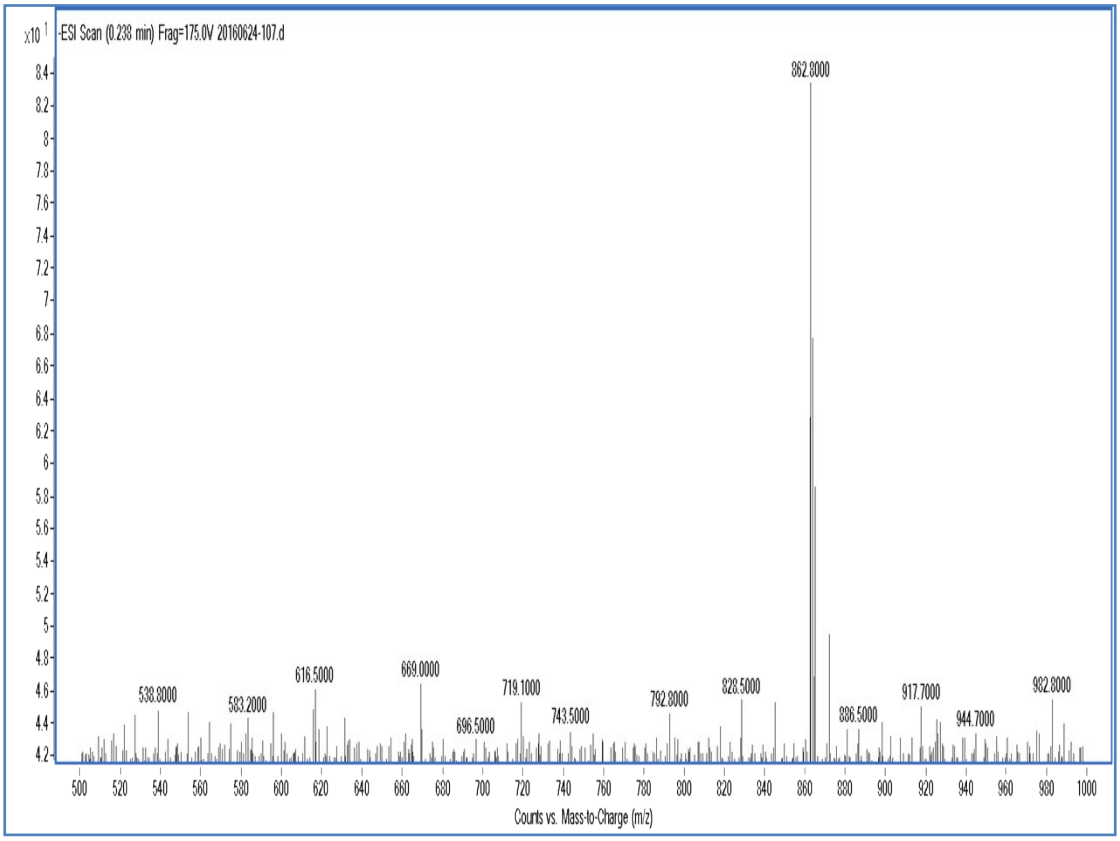


**Figure S20**: The anionic mass spectrum of complex **7** ($BArF^-$).

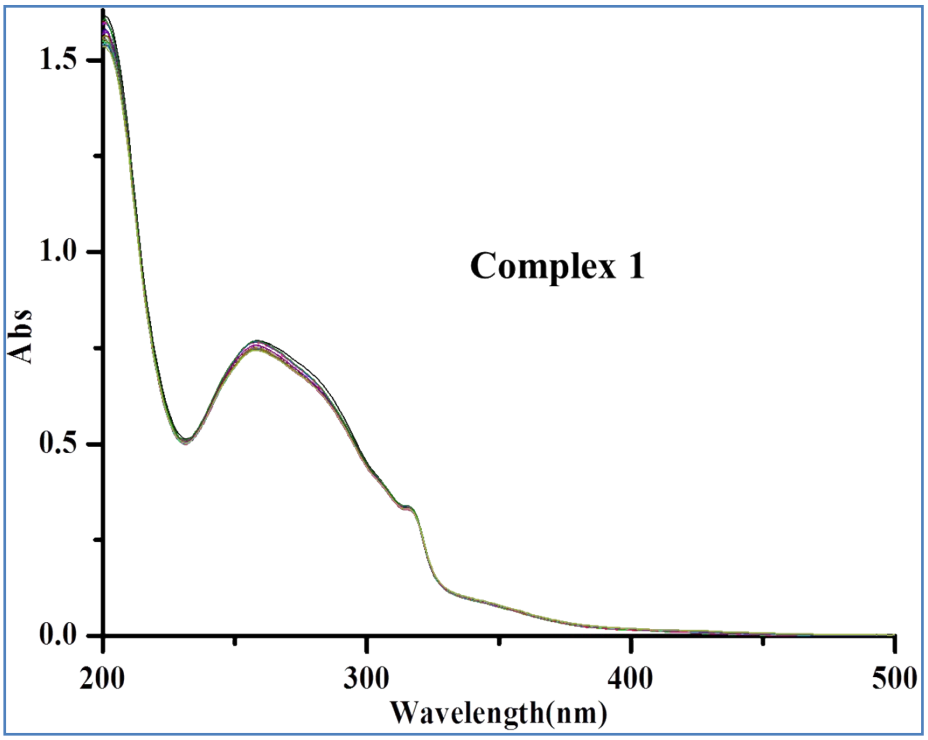


**Figure S21**. UV-Vis spectrum for a 50 μM solution of complex **1** in 10% MeOH/90% $H_2O$ (v/v) recorded over a period of 8 h at 298 K.

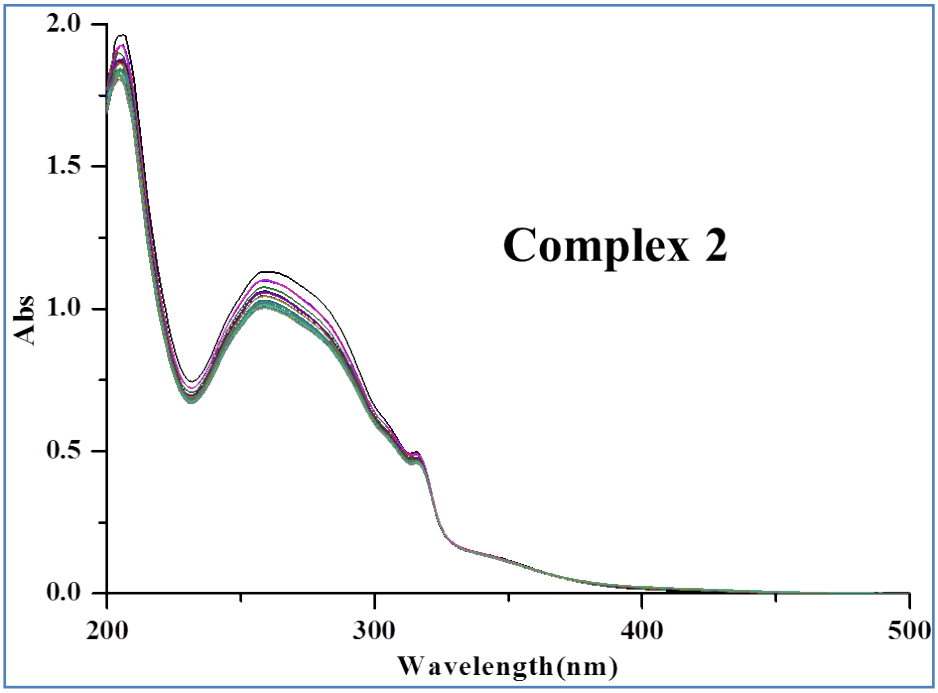


**Figure S22**. UV-Vis spectrum for a 50 μM solution of complex **2** in 10% MeOH/90% $H_2O$ (v/v) recorded over a period of 8 h at 298 K.

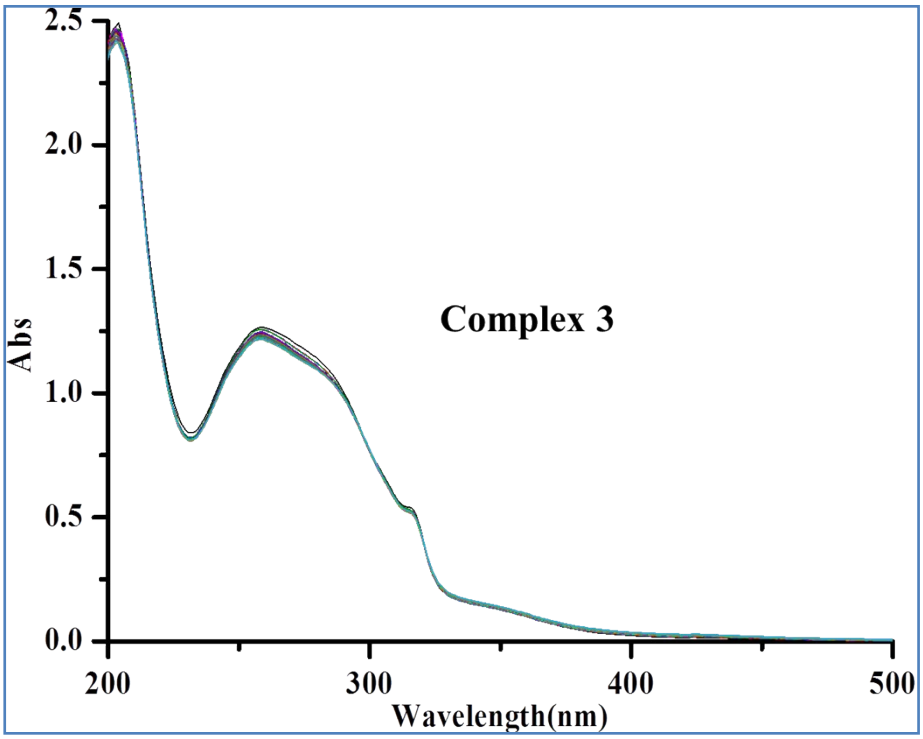


**Figure S23**. UV-Vis spectrum for a 50 μM solution of complex **3** in 10% MeOH/90% $H_2O$ (v/v) recorded over a period of 8 h at 298 K.

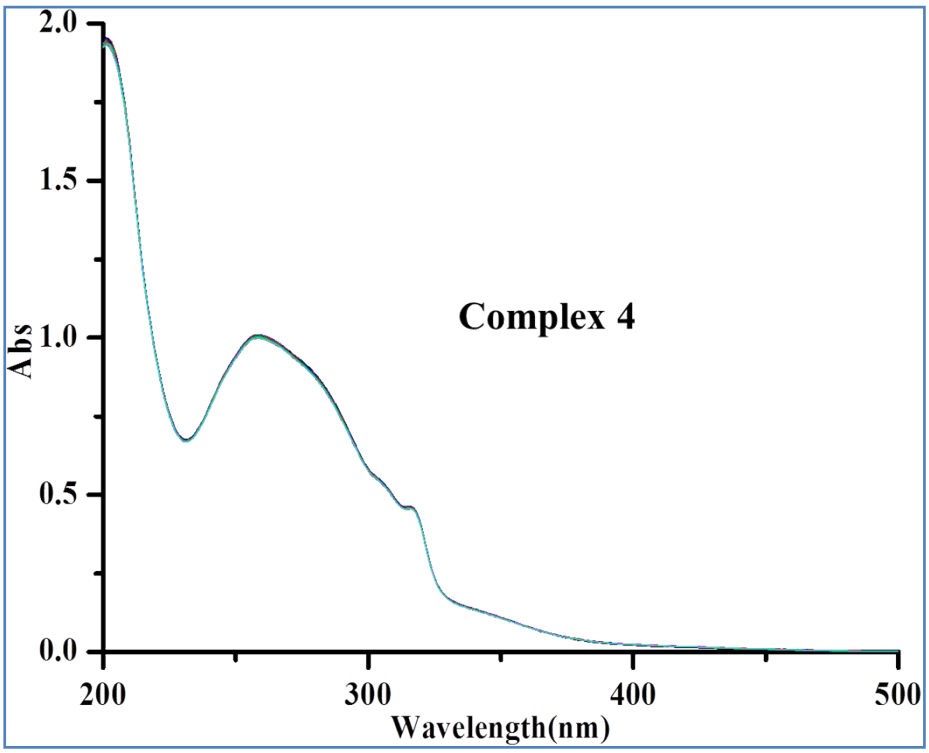


**Figure S24**. UV-Vis spectrum for a 50 μM solution of complex **4** in 10% MeOH/90% $H_2O$ (v/v) recorded over a period of 8 h at 298 K.

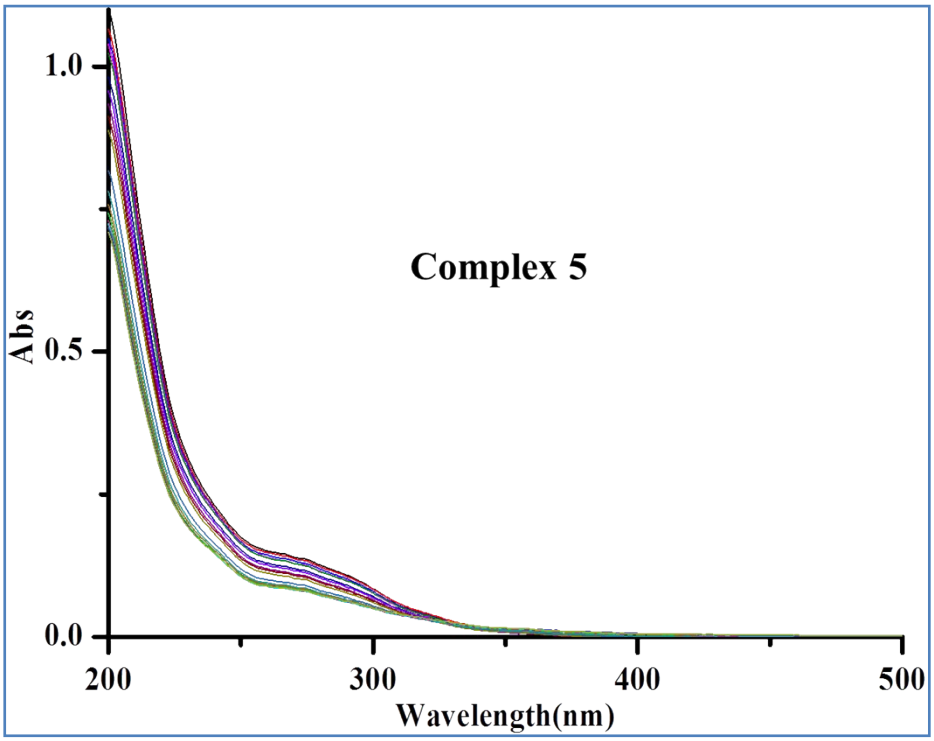


**Figure S25**. UV-Vis spectrum for a 50 μM solution of complex **5** in 10% MeOH/90% $H_2O$ (v/v) recorded over a period of 8 h at 298 K.

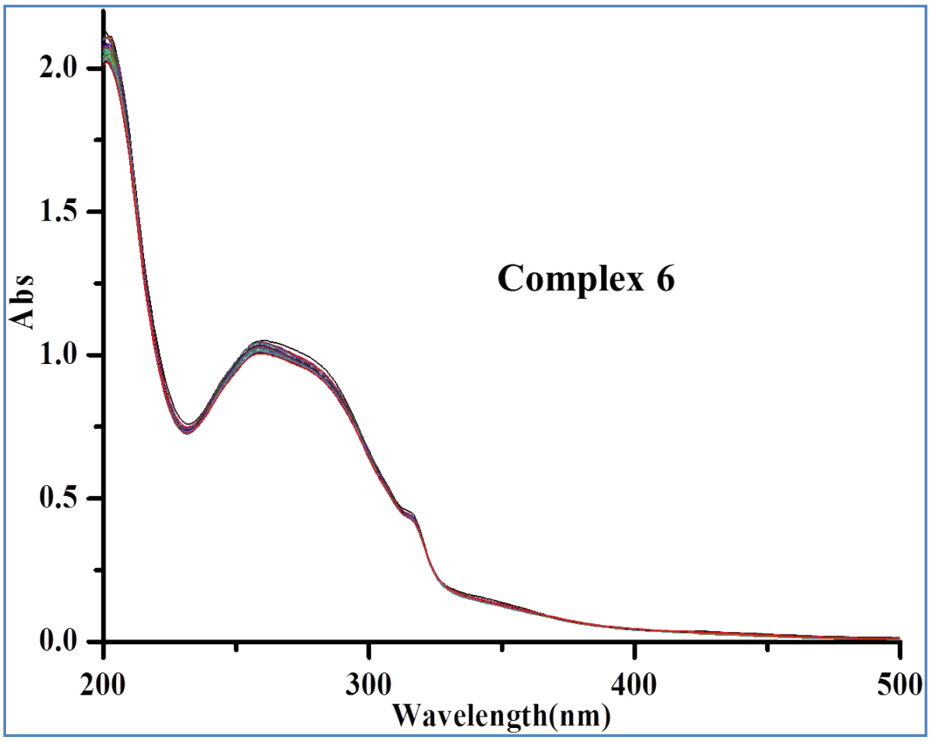


**Figure S26**. UV-Vis spectrum for a 50 μM solution of complex **6** in 10% MeOH/90% $H_2O$ (v/v) recorded over a period of 8 h at 298 K.

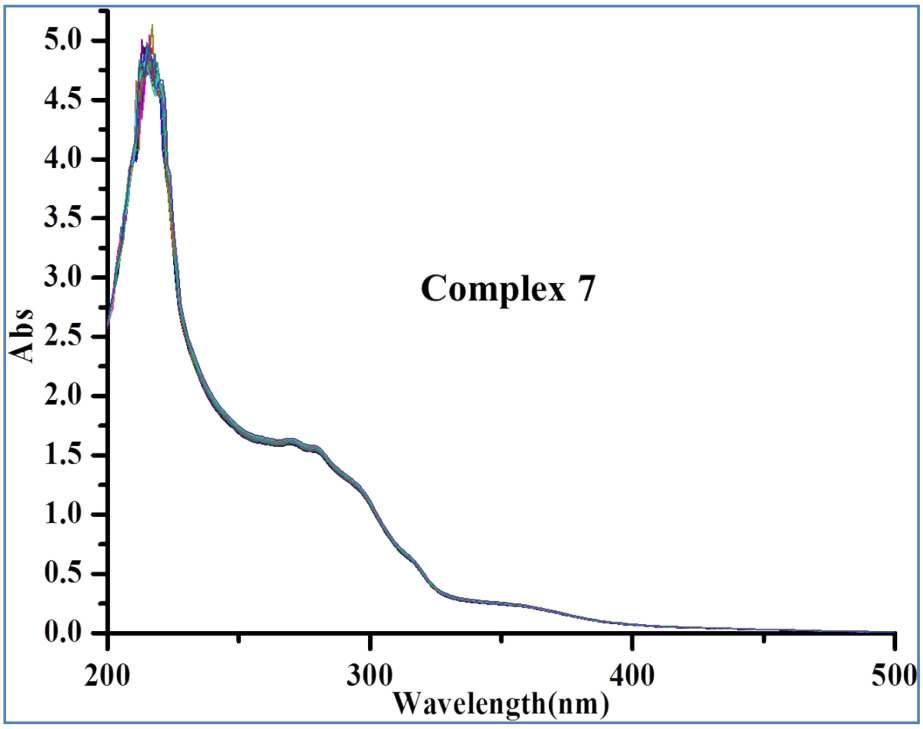


**Figure S27**. UV-Vis spectrum for a 50 μM solution of complex **7** in 10% MeOH/90% $H_2O$ (v/v) recorded over a period of 8 h at 298 K.

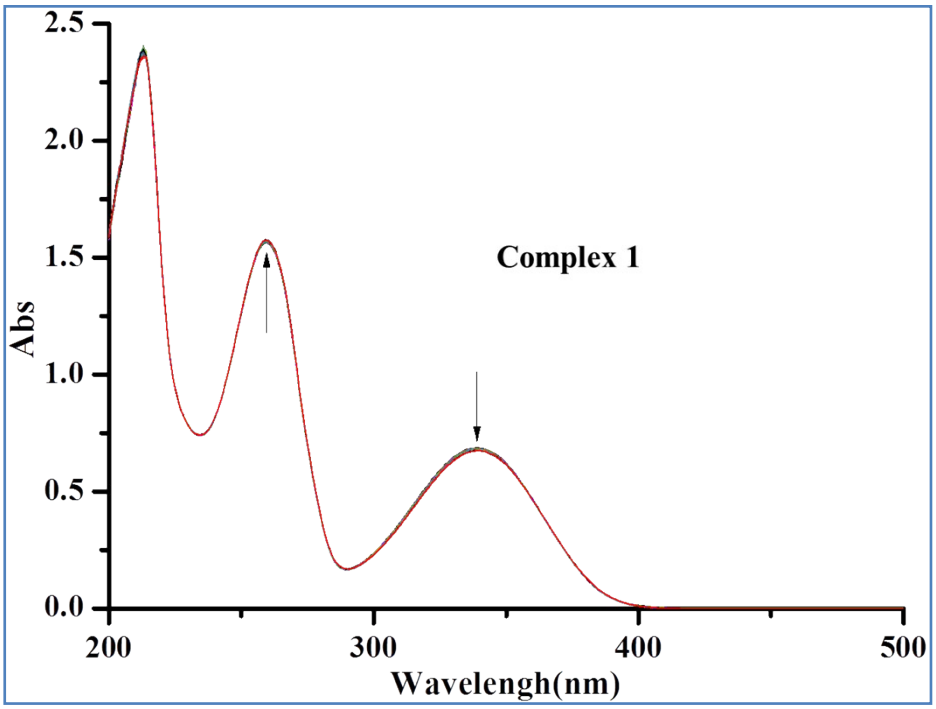


**Figure S28**. UV-Vis spectrum of the reaction of NADH (110 μM) with complex **1** $[Cp^{biph}Ir(bpy)Cl]PF_6$ (1 μM) in 10% MeOH / 90% $H_2O$ (v/v) at 298 K for 8 h.

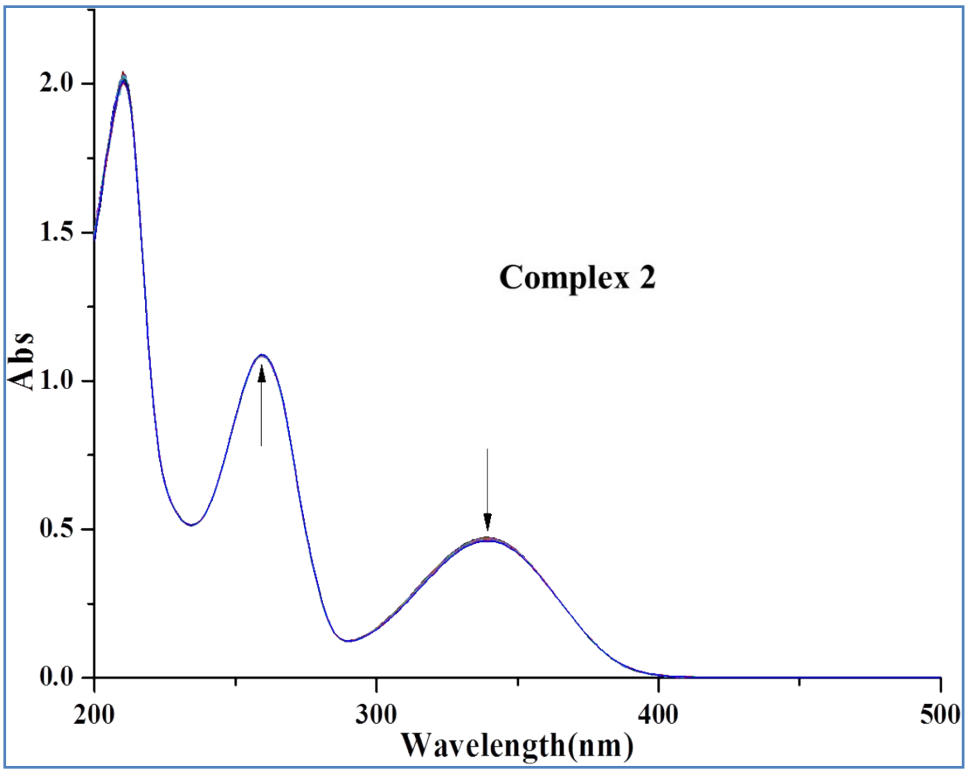


**Figure S29**. UV-Vis spectrum of the reaction of NADH (80 μM) with complex **2** $[Cp^{biph}Ir(bpy)Cl]PF_6$ (1 μM) in 10% MeOH / 90% $H_2O$ (v/v) at 298 K for 8 h.

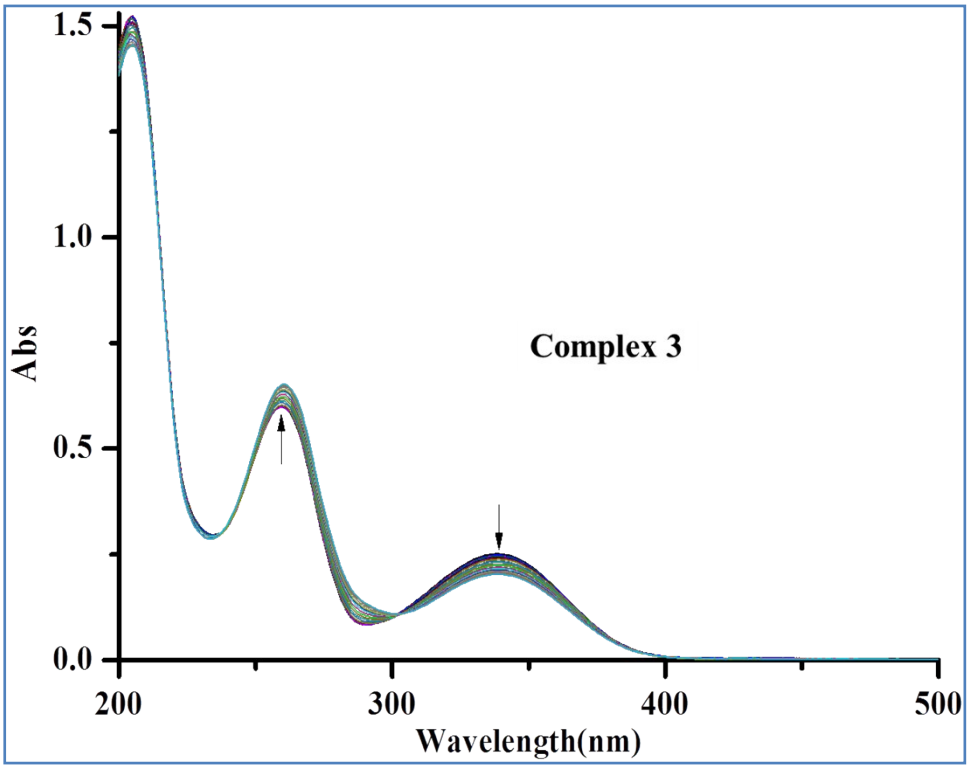


**Figure S30.** UV-Vis spectrum of the reaction of NADH (50 µM) with complex **3** $[Cp^{biph}Ir(bpy)Cl]BF_4$ (1 µM) in 10% MeOH / 90% $H_2O$ (v/v) at 298 K for 8 h.

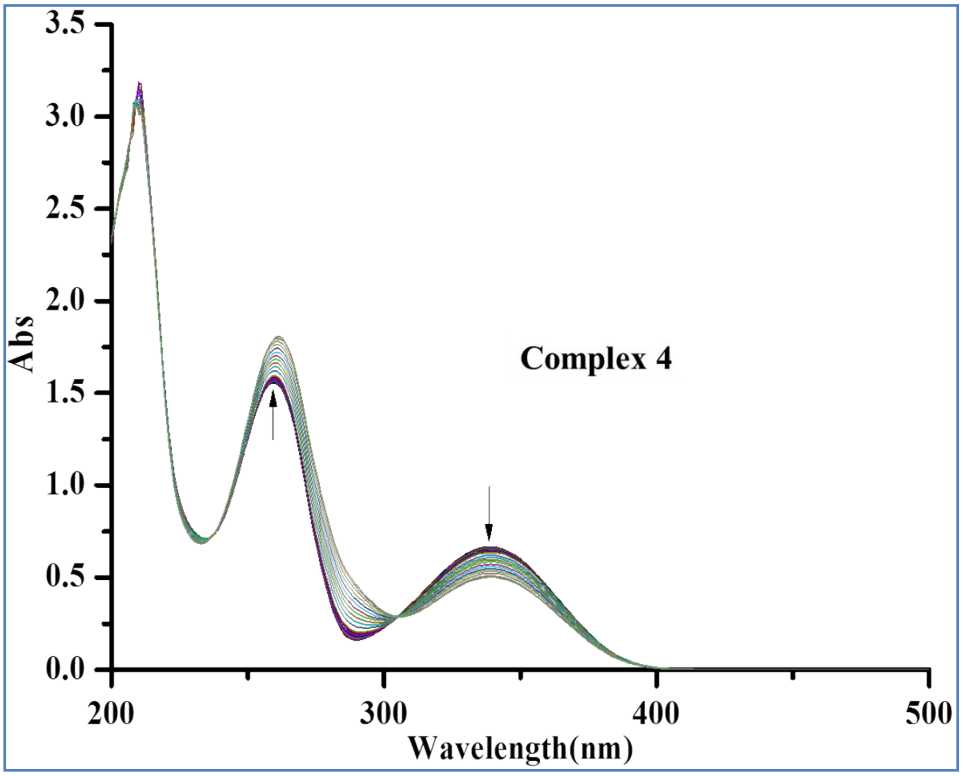


**Figure S31.** UV-Vis spectrum of the reaction of NADH (107 µM) with complex **4** $[Cp^{biph}Ir(bpy)Cl]SbF_6$ (1 µM) in 10% MeOH / 90% $H_2O$ (v/v) at 298 K for 8 h.

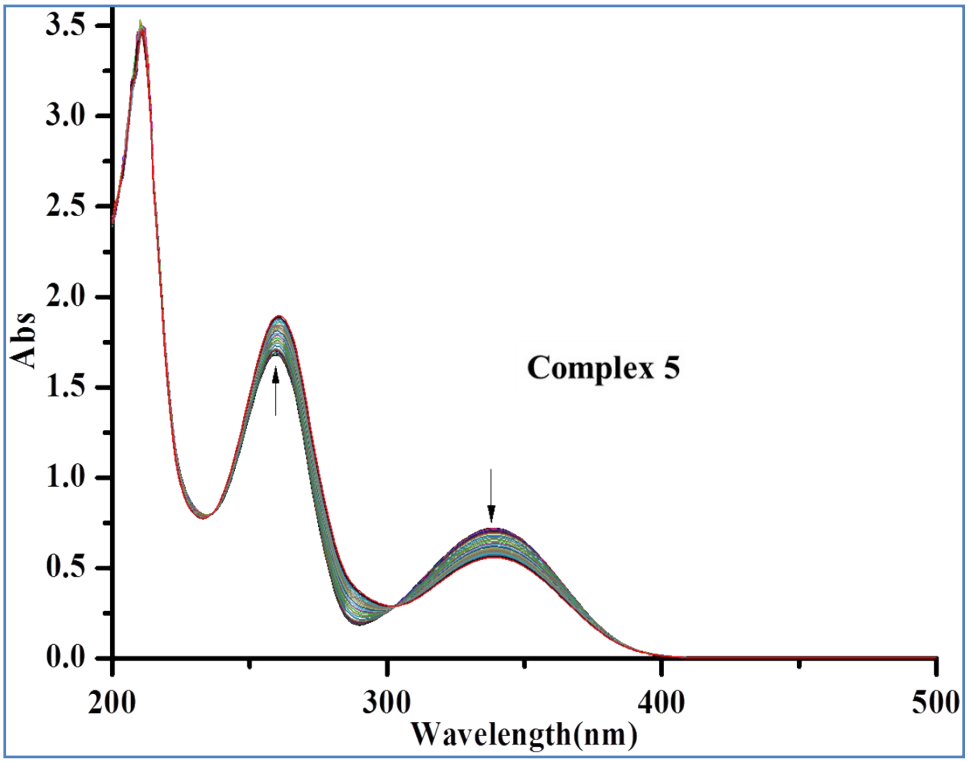


**Figure S32**. UV-Vis spectrum of the reaction of NADH (118 μM) with complex **5** $[Cp^{biph}Ir(bpy)Cl]CF_3SO_3$ (1 μM) in 10% MeOH / 90% $H_2O$ (v/v) at 298 K for 8 h.

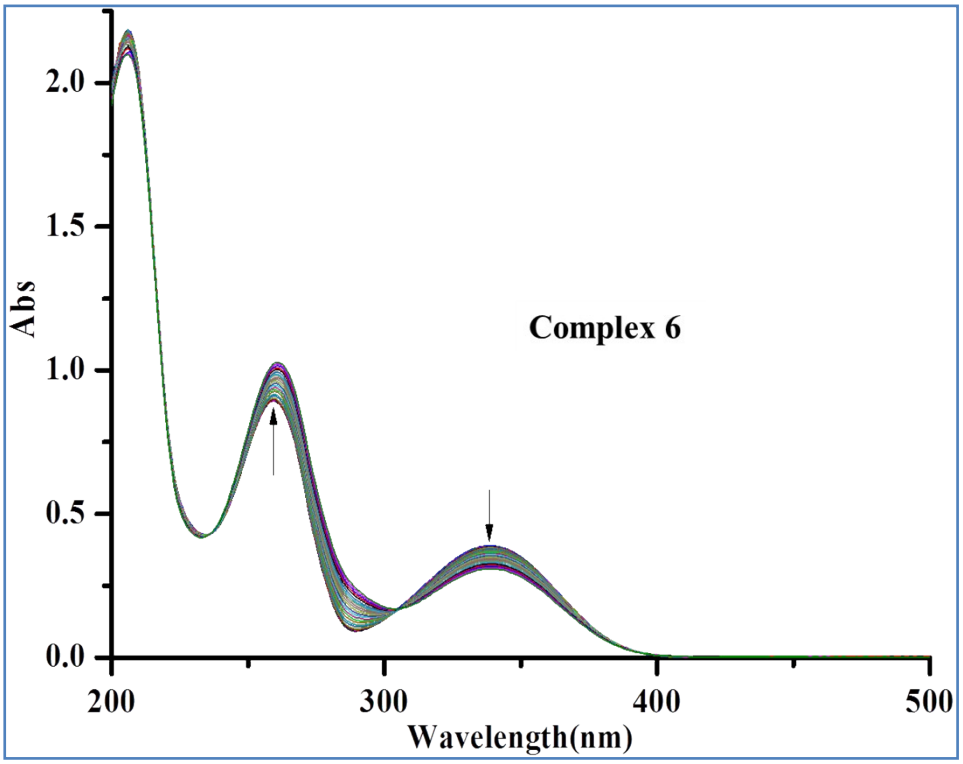


**Figure S33**. UV-Vis spectrum of the reaction of NADH (70 μM) with complex **6** $[Cp^{biph}Ir(bpy)Cl]BPh_4$ (1 μM) in 10% MeOH / 90% $H_2O$ (v/v) at 298 K for 8 h.

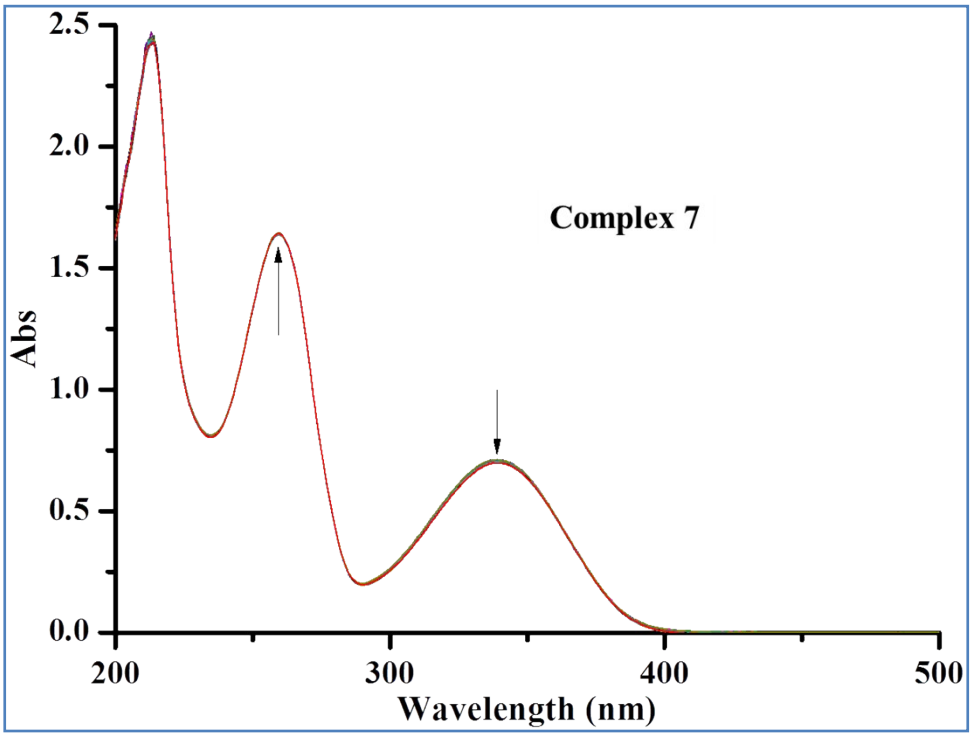


**Figure S34**. UV-Vis spectrum of the reaction of NADH (114 μM) with complex **7** $[Cp^{biph}Ir(bpy)Cl]PF_6$ (1 μM) in 10% MeOH / 90% $H_2O$ (v/v) at 298 K for 8 h.

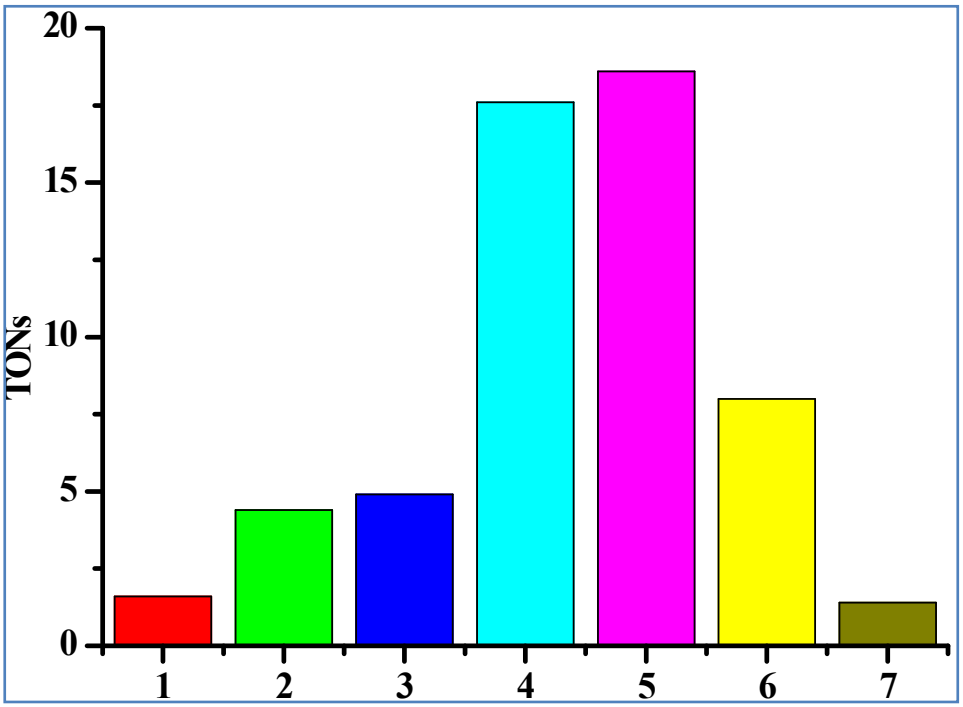


**Figure S35**. The turnover numbers (TONs) of complexes **1**-**7**.